



**HAL**  
open science

## **N<sub>2</sub> fixation in the Mediterranean Sea related to the composition of the diazotrophic community, and impact of dust under present and future environmental conditions.**

Céline Ridame, Julie Dinasquet, Søren Hallstrøm, Estelle Bigeard, Lasse Riemann, France van Wambeke, Matthieu Bressac, Elvira Pulido-Villena, Vincent Taillandier, Frédéric Gazeau, et al.

### ► **To cite this version:**

Céline Ridame, Julie Dinasquet, Søren Hallstrøm, Estelle Bigeard, Lasse Riemann, et al.. N<sub>2</sub> fixation in the Mediterranean Sea related to the composition of the diazotrophic community, and impact of dust under present and future environmental conditions.. *Biogeosciences*, 2022, 19 (2), pp.415-435. 10.5194/bg-19-415-2022 . hal-03853645v2

**HAL Id: hal-03853645**

**<https://hal.science/hal-03853645v2>**

Submitted on 18 Nov 2022

**HAL** is a multi-disciplinary open access archive for the deposit and dissemination of scientific research documents, whether they are published or not. The documents may come from teaching and research institutions in France or abroad, or from public or private research centers.

L'archive ouverte pluridisciplinaire **HAL**, est destinée au dépôt et à la diffusion de documents scientifiques de niveau recherche, publiés ou non, émanant des établissements d'enseignement et de recherche français ou étrangers, des laboratoires publics ou privés.



## N<sub>2</sub> fixation in the Mediterranean Sea related to the composition of the diazotrophic community and impact of dust under present and future environmental conditions

Céline Ridame<sup>1</sup>, Julie Dinasquet<sup>2,3</sup>, Søren Hallstrøm<sup>4</sup>, Estelle Bigeard<sup>5</sup>, Lasse Riemann<sup>4</sup>, France Van Wambeke<sup>6</sup>, Matthieu Bressac<sup>7</sup>, Elvira Pulido-Villena<sup>6</sup>, Vincent Taillandier<sup>7</sup>, Frédéric Gazeau<sup>7</sup>, Antonio Tovar-Sanchez<sup>8</sup>, Anne-Claire Baudoux<sup>5</sup>, and Cécile Guieu<sup>7</sup>

<sup>1</sup>Laboratoire d’Océanographie et du Climat: Expérimentation et Approches Numériques (LOCEAN-IPSL), Sorbonne University, CNRS-IRD-MNHN, 75005 Paris, France

<sup>2</sup>Scripps Institution of Oceanography, University of California San Diego, La Jolla, CA, USA

<sup>3</sup>Sorbonne University, CNRS, Laboratoire d’Océanographie Microbienne, LOMIC, 66650 Banyuls-sur-Mer, France

<sup>4</sup>Marine Biology Section, Department of Biology, University of Copenhagen, 3000 Helsingør, Denmark

<sup>5</sup>Sorbonne University, CNRS, Station Biologique de Roscoff, UMR 7144 Adaptation et Diversité en Milieu Marin, Roscoff, France

<sup>6</sup>Aix-Marseille Université, Université de Toulon, CNRS/INSU, IRD, Mediterranean Institute of Oceanography (MIO), UM 110, 13288, Marseille, France

<sup>7</sup>Sorbonne Université, CNRS, Laboratoire d’Océanographie de Villefranche, LOV, 06230 Villefranche-sur-Mer, France

<sup>8</sup>Department of Ecology and Coastal Management, Institute of Marine Sciences of Andalusia (CSIC), 11510 Puerto Real, Cádiz, Spain

**Correspondence:** Céline Ridame (celine.ridame@locean.ipsl.fr)

Received: 24 July 2021 – Discussion started: 23 August 2021

Revised: 19 November 2021 – Accepted: 30 November 2021 – Published: 25 January 2022

**Abstract.** N<sub>2</sub> fixation rates were measured in the 0–1000 m layer at 13 stations located in the open western and central Mediterranean Sea (MS) during the PEACETIME cruise (late spring 2017). While the spatial variability in N<sub>2</sub> fixation was not related to Fe, P nor N stocks, the surface composition of the diazotrophic community indicated a strong longitudinal gradient increasing eastward for the relative abundance of non-cyanobacterial diazotrophs (NCDs) (mainly  $\gamma$ -Proteobacteria) and conversely decreasing eastward for photo-heterotrophic group A (UCYN-A) (mainly UCYN-A1 and UCYN-A3), as did N<sub>2</sub> fixation rates. UCYN-A4 and UCYN-A3 were identified for the first time in the MS. The westernmost station influenced by Atlantic waters and characterized by highest stocks of N and P displayed a patchy distribution of diazotrophic activity with an exceptionally high rate in the euphotic layer of 72.1 nmol NL<sup>-1</sup> d<sup>-1</sup>, which could support up to 19 % of primary production. At this station at 1 % PAR (photosynthetically available radiation) depth, UCYN-A4 represented up to 94 % of the diazotrophic

community. These in situ observations of greater relative abundance of UCYN-A at stations with higher nutrient concentrations and dominance of NCDs at more oligotrophic stations suggest that nutrient conditions – even in the nanomolar range – may determine the composition of diazotrophic communities and in turn N<sub>2</sub> fixation rates. The impact of Saharan dust deposition on N<sub>2</sub> fixation and diazotrophic communities was also investigated, under present and future projected conditions of temperature and pH during short-term (3–4 d) experiments at three stations. New nutrients from simulated dust deposition triggered a significant stimulation of N<sub>2</sub> fixation (from 41 % to 565 %). The strongest increase in N<sub>2</sub> fixation was observed at the stations dominated by NCDs and did not lead on this short timescale to changes in the diazotrophic community composition. Under projected future conditions, N<sub>2</sub> fixation was either increased or unchanged; in that later case this was probably due to a too-low nutrient bioavailability or an increased grazing pressure. The future warming and acidification likely benefited NCDs (*Pseudomonas*) and

UCYN-A2, while disadvantaged UCYN-A3 without knowing which effect (alone or in combination) is the driver, especially since we do not know the temperature optima of these species not yet cultivated as well as the effect of acidification.

## 1 Introduction

The Mediterranean Sea (MS) is considered to be one of the most oligotrophic regions of the world's ocean (Krom et al., 2004; Bosc et al., 2004). It is characterized by a longitudinal gradient in nutrient availability, phytoplanktonic biomass and primary production (PP) decreasing eastward (Manca et al., 2004; D'Ortenzio and Ribera d'Alcalà, 2009; Ignatiades et al., 2009; Siokou-Frangou et al., 2010; El Hourany et al., 2019). From May to October, the upper water column is well stratified (D'Ortenzio et al., 2005), and the sea surface mixed layer (SML) becomes nutrient-depleted, leading to low PP (e.g., Lazzari et al., 2012). Most measurements of N<sub>2</sub> fixation during the stratified period have shown low rates ( $\leq 0.5 \text{ nmol NL}^{-1} \text{ d}^{-1}$ ) in surface waters of the open MS (Ibello et al., 2010; Bonnet et al., 2011; Yogeve et al., 2011; Ridame et al., 2011; Rahav et al., 2013; Benavides et al., 2016), indicating that N<sub>2</sub> fixation represents a minor source of bioavailable nitrogen in the MS (Krom et al., 2010; Bonnet et al., 2011). These low rates are likely related to the extremely low bioavailability in dissolved inorganic phosphorus (DIP) (Rees et al., 2006; Ridame et al., 2011). The high concentrations of dissolved iron (DFe) in the SML due to accumulated atmospheric Fe deposition (Bonnet and Guieu, 2006; Tovar-Sánchez et al., 2020; Bressac et al., 2021) suggest that the bioavailability of Fe is not a controlling factor of N<sub>2</sub> fixation (Ridame et al., 2011). Occasionally, high N<sub>2</sub> fixation rates have been reported locally in the northwestern ( $17 \text{ nmol NL}^{-1} \text{ d}^{-1}$ ; Garcia et al., 2006) and eastern MS ( $129 \text{ nmol NL}^{-1} \text{ d}^{-1}$ ; Rees et al., 2006). Usually, the low N<sub>2</sub> fixation rates in the Mediterranean offshore waters are associated with low abundance of diazotrophs, mainly dominated by unicellular organisms (Man-Aharonovich et al., 2007; Yogeve et al., 2011; Le Moal et al., 2011). Unicellular diazotrophs from the photo-heterotrophic group A (UCYN-A; Zehr et al., 1998) largely dominated the cyanobacteria assemblage in the MS (Le Moal et al., 2011), and very low concentrations of filamentous diazotrophic cyanobacteria have only been recorded in the eastern basin (Bar-Zeev et al., 2008; Le Moal et al., 2011; Yogeve et al., 2011). The UCYN-A cluster consists of four sublineages – UCYN-A1, UCYN-A2, UCYN-A3 and UCYN-A4 (Thompson et al., 2014; Farnelid et al., 2016; Turk Kubo et al., 2017; Cornejo-Castillo et al., 2019) – of which only UCYN-A1 and UCYN-A2 have been previously detected in the MS (Man-Aharonovich et al., 2007; Martinez-Perez et al., 2016; Pierrela Karlusich et al., 2021). Heterotrophic diazotrophs are widely distributed over the offshore surface waters (Le Moal et al.,

2011), and the decreasing eastward gradient of surface N<sub>2</sub> fixation rate could be related to a predominance of photo-autotrophic diazotrophs in the western basin and a predominance of heterotrophic diazotrophs in the eastern one (Rahav et al., 2013).

The MS is strongly impacted by periodic dust events, originating from the Sahara, which have been recognized as a significant source of macro- and micronutrients to the nutrient-depleted SML during stratified periods (Guieu and Ridame, 2020a and references therein; Mas et al., 2020). Results from Saharan dust seeding experiments during open-sea microcosms and coastal mesocosms in the MS showed stimulation of both PP (Herut et al., 2005; Ternon et al., 2011; Ridame et al., 2014; Herut et al., 2016) and heterotrophic bacterial production (BP) (Pulido-Villena et al., 2008, 2014; Lekunberri et al., 2010; Herut et al., 2016). Experimental Saharan dust seeding was also shown to enhance N<sub>2</sub> fixation in the western and eastern MS (Ridame et al., 2011; Ternon et al., 2011; Ridame et al., 2013; Rahav et al., 2016a) and to alter the composition of the diazotrophic community (Rahav et al., 2016a), as also shown in the tropical North Atlantic (Langlois et al., 2012).

The MS has been identified as one of the primary hotspots for climate change (Giorgi, 2006). Future sea surface warming and associated increase in stratification (Somot et al., 2008) might reinforce the importance of atmospheric inputs as a source of new nutrients for biological activities during that season, including diazotrophic microorganisms. This fertilizing effect could also be enhanced by the expected decline in pH (Mermex Group, 2011), which could increase the nutrient dust solubility in seawater. Under nutrient-repleted conditions, predicted elevated temperature and CO<sub>2</sub> concentration favor the growth and N<sub>2</sub> fixation of the filamentous cyanobacteria *Trichodesmium* and of the photo-autotrophic UCYN-B and UCYN-C (Webb et al., 2008; Hutchins et al., 2013; Fu et al., 2008, 2014; Eichner et al., 2014; Jiang et al., 2018), whereas effects on UCYN-A and non-cyanobacterial diazotrophs (NCDs) are uncertain.

In this context, the first objective of this study is to investigate during the season characterized by strong stratification and low productivity the spatial variability in N<sub>2</sub> fixation rates in relation to nutrient availability and diazotrophic community composition. The second objective was to study, for the first time, the impact of a realistic Saharan deposition event in the open MS on N<sub>2</sub> fixation rates and diazotrophic community composition under present and realistic projected conditions of temperature and pH for 2100.

## 2 Materials and methods

### 2.1 Oceanographic cruise

All data were acquired during the PEACETIME cruise (ProceEss studies at the Air–sEa Interface after dust deposition

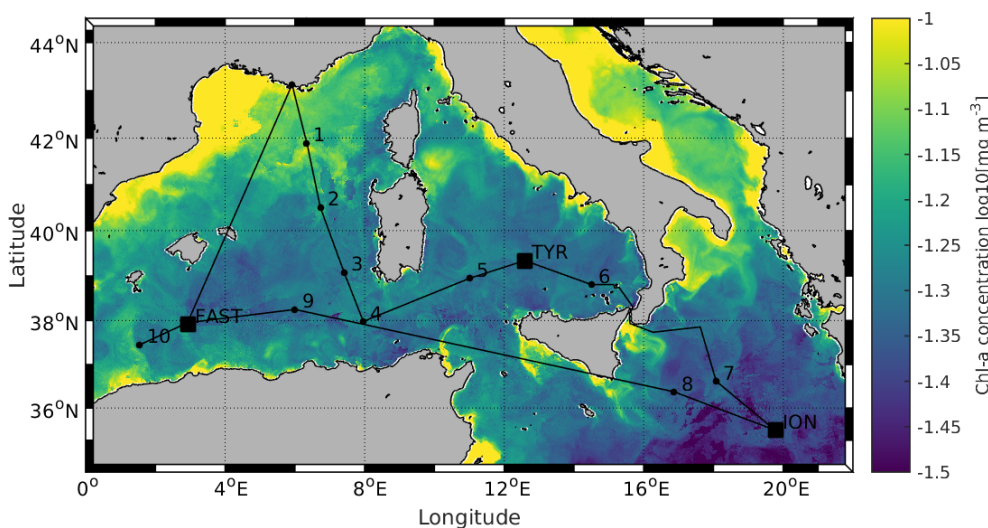


**Figure 1.** Locations of the 10 short (ST1 to ST10) and 3 long stations (TYR, ION and FAST). Stations 1 and 2 were located in the Provencal Basin; Stations 5, 6 and TYR in the Tyrrhenian Sea; Stations 7, 8 and ION in the Ionian Sea; and Stations 3, 4, 9, 10 and FAST in the Algerian Basin. Satellite-derived surface chlorophyll *a* concentration ( $\text{mg m}^{-3}$ ) averaged over the entire duration of the PEACETIME cruise (Courtesy of Louise Rousselet)

in the MEditerranean sea) in the western and central MS on board the R/V *Pourquoi Pas?* from 10 May to 11 June 2017 (<http://peacetime-project.org/>, last access: 17 January 2022) (see the detailed description in Guieu et al., 2020a). The cruise track, including 10 short stations (ST1 to ST10) and 3 long stations (TYR, ION and FAST), is shown in Fig. 1 (coordinates in Table S1 in the Supplement). Stations 1 and 2 were located in the Liguro-Provencal Basin; Stations 5, 6 and TYR in the Tyrrhenian Sea; Stations 7, 8 and ION in the Ionian Sea; and Stations 3, 4, 9, 10 and FAST in the Algerian Basin.

## 2.2 Dust seeding experiments

Experimental dust seedings into six large tanks were conducted at each of the three long stations (TYR, ION and FAST) under present and future conditions of temperature and pH. Based on previous studies, the location of these stations was chosen based on several criteria and because they represent three main bioregions of the MS (Guieu et al., 2020a, their Fig. S1). They are located along the longitudinal gradient in biological activity, including the activity of diazotrophs decreasing eastward (Bonnet et al., 2011; Rahav et al., 2013). The experimental setup is fully described in a companion paper (Gazeau et al., 2021a). Briefly, six climate reactors (volume of about 300 L) made in high-density polyethylene were placed in a temperature-controlled container and covered with a lid equipped with LEDs to reproduce the natural light cycle. The tanks were filled with unfiltered surface seawater collected at  $\sim 5$  m with a peristaltic pump at the end of the day ( $T - 12$  h) before the start of the experiments the next morning (T0). Two replicate tanks were

amended with mineral Saharan dust (dust treatments D1 and D2) simulating a high but realistic atmospheric dust deposition of  $10 \text{ g m}^{-2}$  (Guieu et al., 2010b). Two other tanks were also amended with Saharan dust (same dust flux as in the dust treatment) under warmer ( $\sim +3$  °C) and more acidic water conditions ( $\sim -0.3$  pH unit) (greenhouse treatments G1 and G2). This corresponds to the Intergovernmental Panel on Climate Change (IPCC) projections for 2100 under RCP8.5 (IPCC, 2019). Seawater in G1 and G2 was warmed overnight to reach  $+3$  °C and acidified through the addition of CO<sub>2</sub>-saturated 0.2  $\mu\text{m}$  filtered seawater ( $\sim 1.5$  L in 300 L). The difference in temperature between G (greenhouse) tanks and other tanks (C, controls, and D, dust) was  $+3$ ,  $+3.2$  and  $+3.6$  °C at TYR, ION and FAST, respectively, and the decrease in pH was  $-0.31$ ,  $-0.29$  and  $-0.33$  at TYR, ION and FAST, respectively (Gazeau et al., 2021a). Two tanks were filled with untreated water (Controls C1 and C2). The experiment at TYR and ION lasted 3 d, while the experiment at FAST lasted 4 d. The sampling session took place every morning at the same time over the duration of the experiments.

The fine fraction ( $< 20 \mu\text{m}$ ) of a Saharan soil collected in southern Tunisia used in this study has been previously used for the seeding of mesocosms in the framework of the DUNE project (a DUst experiment in a low-Nutrient, low-chlorophyll Ecosystem). Briefly, the dust was previously subjected to physico-chemical transformations mimicking the mixing between dust and pollution air masses during atmospheric transport (see details in Desboeufs et al., 2001; Guieu et al., 2010b). This dust contained  $0.055 \pm 0.003$  % of P,  $1.36 \pm 0.09$  % of N and  $2.26 \pm 0.03$  % of Fe in weight (Desboeufs et al., 2014). Right before the artificial seeding, the

**Table 1.** Integrated N<sub>2</sub> fixation over the surface mixed layer (SML; from surface to the mixed layer depth), from the surface to the base of the euphotic layer (1 % PAR depth), over the aphotic layer (1 % PAR depth to 1000 m) and from the surface to 1000 m at all the sampled stations. Contribution (in percent) of SML-integrated N<sub>2</sub> fixation to euphotic-layer-integrated N<sub>2</sub> fixation and contribution of euphotic-layer-integrated N<sub>2</sub> fixation to total (0–1000 m) integrated N<sub>2</sub> fixation.

	N <sub>2</sub> Fix <sub>SML</sub> μmol N m <sup>-2</sup> d <sup>-1</sup>	N <sub>2</sub> Fix <sub>euphotic</sub> μmol N m <sup>-2</sup> d <sup>-1</sup>	N <sub>2</sub> Fix <sub>aphotic</sub> μmol N m <sup>-2</sup> d <sup>-1</sup>	N <sub>2</sub> Fix <sub>0-1000 m</sub> μmol N m <sup>-2</sup> d <sup>-1</sup>	N <sub>2</sub> Fix <sub>SML</sub> / N <sub>2</sub> Fix <sub>euphotic</sub> %	N <sub>2</sub> Fix <sub>euphotic</sub> / N <sub>2</sub> Fix <sub>0-1000 m</sub> %
ST01	14.6	42.6	56.5	99.1	34	43
ST02	10.7	36.0	16.0	51.9	30	69
ST03	7.8	58.3	18.1	76.4	13	76
ST04	10.8	46.6	38.5	85.1	23	55
ST05	4.9	46.3	36.1	82.4	10	56
TYR	4.2	38.6	53.0	91.6	11	42
ST06	9.1	34.9	29.8	64.7	26	54
ST07	10.5	43.5	55.4	98.8	24	44
ION	6.2	40.6	56.5	97.1	15	42
ST08	4.3	27.0	12.3	39.3	16	69
ST09	3.4	50.2	43.3	93.5	7	54
FAST	5.9	58.2	35.7	93.8	10	62
ST10	13.7	1908	63.7	1972	1	97
Mean ± SD (ST10 excluded)	7.7 ± 3.5	44 ± 9	38 ± 16	81 ± 20	18 % ± 9 %	55 % ± 12 %
Mean ± SD (all stations)	8.2 ± 3.7	187 ± 517	40 ± 17	227 ± 525	17 % ± 10 %	59 % ± 16 %

dust was mixed with 2 L of ultrapure water in order to mimic a wet deposition event and sprayed at the surface of the climate reactors D and G. The succession of operations is fully described in Gazeau et al. (2021a; see their Table 1).

### 2.3 N<sub>2</sub> fixation and primary production

All materials were acid-washed (HCl Suprapur 32 %) following trace metal clean procedures. Before sampling, bottles were rinsed three times with the sampled seawater. For the in situ measurements, seawater was sampled using a trace metal clean (TMC) rosette equipped with 24 GO-FLO bottles (Guieu et al., 2020a). At each station, seven to nine depths were sampled between the surface and 1000 m for N<sub>2</sub> fixation measurements and five depths between surface and ~ 100 m for primary production measurements (one sample per depth). During the seeding experiments, the six tanks were sampled for simultaneous determination of net N<sub>2</sub> and CO<sub>2</sub> fixation rates before dust seeding (initial time T0) and 1 d (T1), 2 d (T2) and 3 d (T3) after dust addition at TYR and ION stations. At FAST, the last sampling took place 4 d (T4) after dust addition.

After collection, 2.3 L of seawater was immediately filtered onto pre-combusted GF/F (glass microfiber) filters to determine natural concentrations and isotopic signatures of particulate organic carbon (POC) and particulate nitrogen (PN). Net N<sub>2</sub> fixation rates were determined using the <sup>15</sup>N<sub>2</sub> gas tracer addition method (Montoya et al., 1996) and net primary production using the <sup>13</sup>C tracer addition method

(Hama et al., 1983). Immediately after sampling, 1 mL of NaH<sup>13</sup>CO<sub>3</sub> (99 %, Eurisotop) and 2.5 mL of 99 % <sup>15</sup>N<sub>2</sub> (Eurisotop) was introduced to 2.3 L polycarbonate bottles through a butyl septum for simultaneous determination of N<sub>2</sub> and CO<sub>2</sub> fixation. <sup>15</sup>N<sub>2</sub> and <sup>13</sup>C tracers were added to obtain a ~ 10 % final enrichment. Then, each bottle was vigorously shaken before incubation for 24 h. The in situ samples from the euphotic zone were incubated in on-deck containers with circulating seawater, equipped with blue filters with different sets of blue neutral density filters (LEE Filters) (percentages of attenuation: 70, 52, 38, 25, 14, 7, 4, 2 and 1 %) to simulate an irradiance level (% PAR) as close as possible to the one corresponding to their depth of origin. Samples for N<sub>2</sub> fixation determination in the aphotic layer were incubated in the dark in thermostated incubators set at in situ temperature. In situ <sup>13</sup>C PP will not be discussed in this paper as <sup>14</sup>C PP rates are presented in Maranon et al. (2021) (see details in Fig. S1 in the Supplement). The in situ <sup>13</sup>C PP and molar C : N ratio in the organic particulate matter, measured simultaneously in our samples (see below for details), were used to estimate the contribution of N<sub>2</sub> fixation to PP.

Samples from the dust addition experiments were incubated in two tanks dedicated to incubation: one tank at the same temperature and irradiance as the C and D tanks and another one at the same temperature and irradiance as the G tanks. It should be noted that <sup>14</sup>C PP was also measured during the seeding experiments (Gazeau et al., 2021b; Fig. S1 in the Supplement).

After 24 h incubation, 2.3 L was filtered onto pre-combusted 25 mm GF/F filters, and filters were stored at  $-25^{\circ}\text{C}$ . Filters were then dried at  $40^{\circ}\text{C}$  for 48 h before analysis. POC and PN as well as  $^{15}\text{N}$  and  $^{13}\text{C}$  isotopic ratios were quantified using an online continuous flow elemental analyzer (Flash 2000 HT) coupled with an isotopic ratio mass spectrometer (Delta V Advantage via a ConFlow IV interface from Thermo Fisher Scientific). For each sample, POC (in the 0–100 m layer) and PN (0–1000 m) were higher than the analytically determined detection limit of  $0.15\ \mu\text{mol}$  for C and  $0.11\ \mu\text{mol}$  for N. Standard deviations were  $0.0007\ \text{at.}\%$  and  $0.0005\ \text{at.}\%$  for  $^{13}\text{C}$  and  $^{15}\text{N}$  enrichment, respectively. The atomic percent excess of the dissolved inorganic carbon (DIC) was calculated by using measured DIC concentrations at the LOCEAN laboratory (SNAPO-CO<sub>2</sub>). N<sub>2</sub> fixation rates were calculated by isotope mass balance equations as described by Montoya et al. (1996). For each sample, the  $^{13}\text{C}$  and  $^{15}\text{N}$  uptake rates were considered to be significant when excess enrichment of POC and PN was greater than 3 times the standard deviation obtained on natural samples. According to our experimental conditions, the minimum detectable  $^{13}\text{C}$  and  $^{15}\text{N}$  uptake rates in our samples were  $5\ \text{nmol}\ \text{CL}^{-1}\ \text{d}^{-1}$  and  $0.04\ \text{nmol}\ \text{NL}^{-1}\ \text{d}^{-1}$ , respectively. CO<sub>2</sub> uptake rates were above the detection limit in the upper 0–100 m, while N<sub>2</sub> fixation was not quantifiable below 300 m depth except at Stations 1 and 10 with rates of  $\sim 0.05\ \text{nmol}\ \text{NL}^{-1}\ \text{d}^{-1}$  at 500 m depth. From these measurements, the molar C : N ratio in the organic particulate matter was calculated and used to estimate the contribution of N<sub>2</sub> fixation to primary production. As a rough estimate of the potential impact of bioavailable N input from N<sub>2</sub> fixation on BP, we used the BP rates presented in companion papers (Gazeau et al., 2021b; Van Wambeke et al., 2021) and converted them to N demand using the molar ratio C : N of 6.8 (Fukuda et al., 1998). Trapezoidal method was used to calculate integrated rates over the SML, the euphotic layer (from surface to 1 % photosynthetically available radiation (PAR) depth) and the 0–1000 m water column.

It must be noted that N<sub>2</sub> fixation rates measured by the  $^{15}\text{N}_2$  tracer gas addition method may have been underestimated due to incomplete  $^{15}\text{N}_2$  gas bubble equilibration (Mohr et al., 2010). However, this potential underestimation is strongly lowered during long incubation (24 h).

The relative changes (RC, in percent) in N<sub>2</sub> fixation in the dust experiments were calculated as follows:

$$\text{RC}(\%) = 100 \cdot \frac{(\text{N}_2\text{FIXATION}_{\text{Tx}} - \text{N}_2\text{FIXATION}_{\text{Control}})}{(\text{N}_2\text{FIXATION}_{\text{Control}})}, \quad (1)$$

with  $\text{N}_2\text{FIXATION}_{\text{Tx}}$  the rate in D1, D2, G1 or G2 at Tx;  $\text{N}_2\text{FIXATION}_{\text{Control}}$  the mean of the duplicated controls (C1 and C2) at Tx; and Tx the time of the sampling.

## 2.4 Composition of the diazotrophic community

Samples for characterization of the diazotrophic communities were collected during the dust seeding experiments in the six tanks at initial time before seeding (T0) and final time (T3 at TYR and ION and T4 at FAST); 3 L of water was collected in acid-washed containers from each tank, filtered onto  $0.2\ \mu\text{m}$  PES (polyethersulfone) filters (Sterivex) and stored at  $-80^{\circ}\text{C}$  until DNA extraction. The composition of the diazotrophic community was also determined at four depths (10, 61, 88 and 200 m) at Station 10. Here, 2 L seawater was collected from the TMC rosette. Immediately after collection, seawater was filtered under low vacuum pressure through a  $0.2\ \mu\text{m}$  nuclepore membrane and stored at  $-80^{\circ}\text{C}$  in cryovials. Nucleic acids were obtained from both filter types using phenol-chloroform extraction followed by purification (NucleoSpin<sup>®</sup> PlantII kit; Macherey-Nagel). DNA extracts were used as templates for PCR (polymerase chain reaction) amplification of the *nifH* gene by nested PCR protocol as fully described in Bigeard et al. (2021; protocol.io). Following polymerase chain reactions, DNA amplicons were purified and quantified using NanoQuant Plate<sup>™</sup> and Tecan Spark<sup>®</sup> (Tecan Trading AG, Switzerland). Each PCR product was normalized to  $30\ \text{ng}\ \mu\text{L}^{-1}$  in the final  $50\ \mu\text{L}$  and sent to Genotoul (<https://www.genotoul.fr/>, last access: 17 January 2022; Toulouse, France) for high-throughput sequencing using paired-end 2x250bp Illumina MiSeq. All reads were processed using the Quantitative Insight Into Microbial Ecology 2 pipeline (QIIME2 v2020.2; Bolyen et al., 2019). Reads were truncated to 350 bp based on sequencing quality, denoised, merged and chimera-checked using DADA2 (Callahan et al., 2016). A total of 1 029 778 reads were assigned to 635 amplicon sequence variants (ASVs). The table was rarefied by filtering at 1 % relative abundance per sample cut-off that reduced the dataset to 97 ASVs, accounting for 98.27 % of all reads. Filtering for homologous genes was done using the NifMAP pipeline (Angel et al., 2018) and translation into amino acids using FrameBot (Wang et al., 2013). This yielded 235 ASVs, accounting for 1 022 184 reads (99 %). These remaining ASVs were classified with DIAMOND blastp (Buchfink et al., 2015) using a FrameBot translated *nifH* database (phylum level version; Moynihan, 2020) based on the ARB database from the Zehr Lab (version June 2017; <https://www.jzehrlab.com/nifh>, last access: 17 January 2022). NifH cluster and subcluster designations were assigned according to Frank et al. (2016). UCYN-A sublineages were assigned by comparison to UCYN-A reference sequences (Farnelid et al., 2016; Turk-Kubo et al., 2017). All sequences associated with this study have been deposited under the BioProject ID PRJNA693966. Alpha and beta diversity indices for community composition were estimated after randomized subsampling. Analyses were run in QIIME 2 and in the Primer v.6 software package (Clarke and Warwick, 2001).

**Table 2.** Initial physico-chemical and biological properties of surface seawater before the perturbation in the dust seeding experiments at TYR, ION and FAST (average at T0 in C and D treatments ( $n = 4$ ) or value at  $T - 12$  h ( $n = 1$ ) in the pumped surface waters). The relative abundances of diazotrophic cyanobacteria and NCDs (non-cyanobacterial diazotrophs) are given as proportion of total *nifH* sequence reads. DIP: dissolved inorganic phosphorus; DFe: dissolved iron. The C : N ratio corresponds to the ratio in the organic particulate matter from IRMS (isotopic ratio mass spectrometer) measurements ( $> 0.7 \mu\text{m}$ ). Means that did not differ significantly between the experiments ( $p > 0.05$ ) are labeled with the same letter (in parentheses).

	TYR	ION	FAST
Day of sampling	1 May 2017	25 May 2017	2 Jun 2017
Temperature ( $^{\circ}\text{C}$ ) <sup>1</sup>	20.6	21.2	21.5
Salinity <sup>1</sup>	37.96	39.02	37.07
<sup>13</sup> C primary production ( $\text{mg C m}^{-3} \text{d}^{-1}$ )	1.23 ± 0.64 (A)	2.53 ± 0.40 (B)	2.82 ± 0.55 (B)
N <sub>2</sub> fixation ( $\text{nmol N L}^{-1} \text{d}^{-1}$ )	0.19 ± 0.03 (A)	0.21 ± 0.05 (A)	0.51 ± 0.04 (B)
Relative abundance of diazotrophic cyanobacteria (%)	4.7 ± 3.8 (A)	6.2 ± 6.5 (A)	91.4 ± 6.0 (B)
Relative abundance of NCDs (%)	95.3 ± 3.9 (A)	93.8 ± 6.5 (A)	8.6 ± 6.0 (B)
Heterotrophic bacterial production ( $\text{ng CL}^{-1} \text{h}^{-1}$ )	26.6 ± 7.0 (AB)	25.9 ± 0.9 (A)	36.3 ± 1.2 (B)
C : N ( $\text{mol mol}^{-1}$ )	9.6 ± 0.8 (A)	10.2 ± 0.8 (A)	9.1 ± 0.5 (A)
DIP (nM) <sup>1</sup>	17	7	13
NO <sub>3</sub> <sup>-</sup> (nM) <sup>1</sup>	14	18	59
NO <sub>3</sub> <sup>-</sup> : DIP ( $\text{mol mol}^{-1}$ )	0.8	2.6	4.5
DFe (nM) <sup>2</sup>	1.5 ± 0.1 (A)	2.6 ± 0.2 (B)	1.8 ± 0.2 (A)

<sup>1</sup> From Gazeau et al. (2021a); <sup>2</sup> from Roy-Barman et al. (2021).

## 2.5 Complementary data from PEACETIME companions papers

**Bacterial production.** Heterotrophic bacterial production (BP; sensu stricto referring to prokaryotic heterotrophic production) was determined on board using the microcentrifuge method with the <sup>3</sup>H-leucine (<sup>3</sup>H-Leu) incorporation technique to measure protein production (Smith and Azam, 1992). The detailed protocol and the rates of BP are presented in Van Wambeke et al. (2021) for measurements in the water column and in Gazeau et al. (2021b) for measurements over the course of the dust seeding experiments.

**Dissolved Fe.** Dissolved iron (DFe) concentrations ( $< 0.2 \mu\text{m}$ ) were measured by flow injection analysis with online preconcentration and chemiluminescence detection (FIA-CL). The detection limit was 15 pM (Bressac et al., 2021). DFe concentrations in the water column along the whole transect are presented in Bressac et al. (2021) and for the dust seeding experiments in Roy-Barman et al. (2021).

**Dissolved inorganic phosphorus and nitrate.** Concentrations of DIP and nitrate (NO<sub>3</sub><sup>-</sup>) were analyzed immediately after collection on  $0.2 \mu\text{m}$  filtered seawater using a segmented flow analyzer (AAIII HR Seal Analytical) according to Aminot and K erouel (2007) with respective detection limits of 0.02 and  $0.05 \mu\text{mol L}^{-1}$ . Samples with concentrations below the limit of detection with standard analysis were analyzed by spectrophotometry using a 2.5 m long waveguide capillary cell (LWCC) for DIP (Pulido-Villena et al., 2010) and a 1 m LWCC for NO<sub>3</sub><sup>-</sup> (Louis et al., 2015); the limit of detection was 1 nM for DIP and 6 nM for NO<sub>3</sub><sup>-</sup>. Samples for determination of NO<sub>3</sub><sup>-</sup> at the nanomolar level were

lost from Stations 1 to 4. The dust addition experiment data are detailed in Gazeau et al. (2021a). The water column data are fully discussed in Pulido-Villena et al. (2021) and Van Wambeke et al. (2021).

## 2.6 Statistical analysis

Pearson's correlation coefficient was used to test the statistical linear relationship ( $p < 0.05$ ) between N<sub>2</sub> fixation and other variables (BP, PP, DFe, DIP, NO<sub>3</sub><sup>-</sup>); it should be noted that the DIN stocks estimated at Stations 1 to 4 (Table S1) were excluded from statistical analysis. In the dust seeding experiments, means at initial time (T0) before dust amendment (average at T0 in C and D treatments,  $n = 4$ ; see Table 2) were compared using a one-way ANOVA followed by a Tukey means comparison test ( $\alpha = 0.05$ ). When assumptions for ANOVA were not respected, means were compared using a Kruskal–Wallis test and a post hoc Dunn test. To test significant differences ( $p < 0.05$ ) between the slopes of N<sub>2</sub> fixation as a function of time in the C, D and G treatments ( $n = 8$ ), an ANCOVA was performed on data presenting a significant linear relationship with time (Pearson's correlation coefficient,  $p < 0.05$ ). Statistical tests were done using XLSTAT and R (version 4.1.1 with the stats, tidyverse and FactoMineR packages).



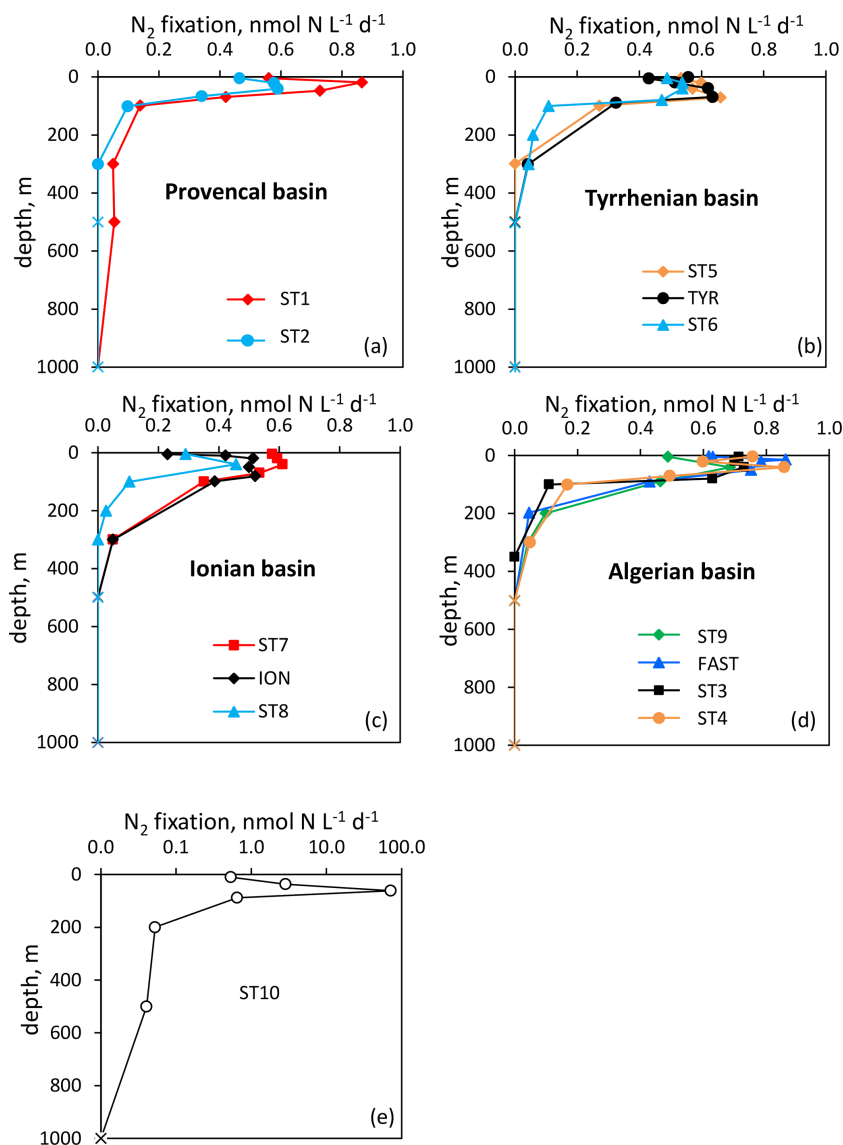


**Figure 2.** Vertical distribution of N<sub>2</sub> fixation (in nmolNL<sup>-1</sup>d<sup>-1</sup>) in the Provencal (a), Tyrrhenian (b), Ionian (c) and Algerian (d) basins and at Station 10 (e). N<sub>2</sub> fixation rates at Station 10 are plotted in log scale because of the high fluxes. Rates under the detection limit (<0.04 nmolNL<sup>-1</sup>d<sup>-1</sup>) are symbolized by crosses.

### 3 Results

#### 3.1 In situ N<sub>2</sub> fixation

##### 3.1.1 Vertical and longitudinal distribution of N<sub>2</sub> fixation

Over the cruise, the water column was well stratified with a shallow SML varying from 7 to 21 m depth (Table S1). Detectable N<sub>2</sub> fixation rates in the 0–1000 m layer ranged from 0.04 to an exceptionally high rate of 72.1 nmolNL<sup>-1</sup>d<sup>-1</sup> at Station 10 (Fig. 2). Vertical N<sub>2</sub> fixation profiles exhibited a similar shape at all stations, with maximum values within the euphotic layer and undetectable values be-

low 300 m depth (except at Stations 1 and 10, with rates of ~0.05 nmolNL<sup>-1</sup>d<sup>-1</sup> at 500 m depth). Within the euphotic layer, all the rates were well above the detection limit (DL=0.04 nmolNL<sup>-1</sup>d<sup>-1</sup>, minimum in situ N<sub>2</sub> fixation=0.22 nmolNL<sup>-1</sup>d<sup>-1</sup>). The highest rates were generally found below the SML and the lowest at the base of the euphotic layer or within the SML (Fig. 2). The lowest N<sub>2</sub> fixation rates integrated over the euphotic and aphotic (defined as 1 % PAR depth to 1000 m) layers were found at Station 8 and the highest at Station 10 (Table 1). On average, 59 ± 16 % of N<sub>2</sub> fixation (min 42 % at TYR and ION, max 97 % at Station 10) took place within the euphotic layer (Table 1). The contribution of the SML-integrated N<sub>2</sub> fixation to



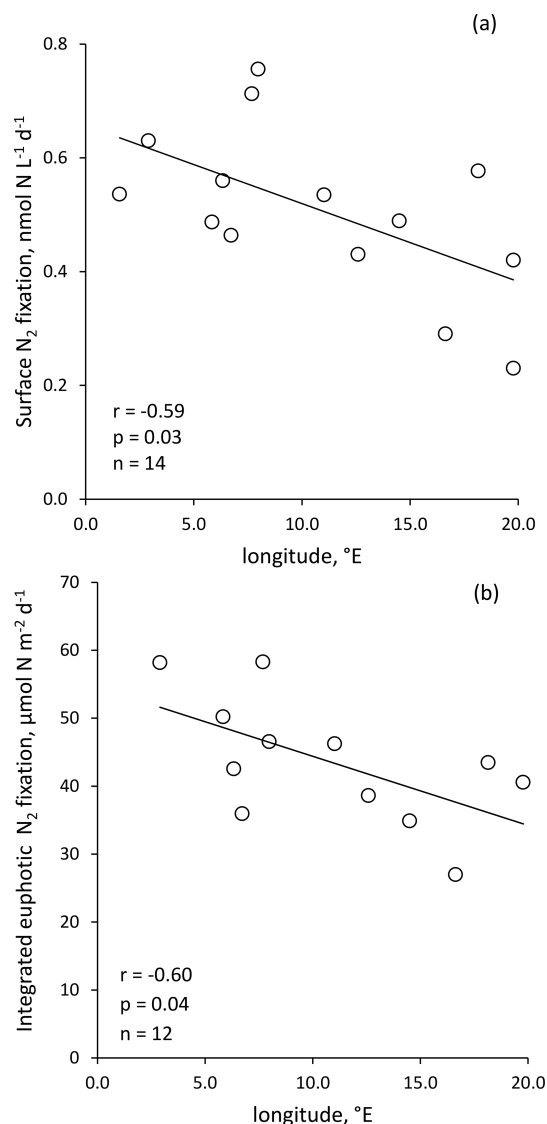


**Figure 3.** Volumetric surface ( $\sim 5$  m) (a) and integrated N<sub>2</sub> fixation from surface to euphotic layer depth (b) along the longitudinal PEACETIME transect (Station 10 was excluded). Integrated N<sub>2</sub> fixation rate from Station 10 was excluded from statistical analysis.

the euphotic-layer-integrated N<sub>2</sub> fixation was low, on average  $17 \pm 10$  %.

Volumetric surface ( $\sim 5$  m) and euphotic-layer-integrated N<sub>2</sub> fixation rates exhibited a longitudinal gradient decreasing eastward ( $r = -0.59$  and  $r = -0.60$ ,  $p < 0.05$ , respectively) (Fig. 3). Integrated N<sub>2</sub> fixation rates over the SML, aphotic and 0–1000 m layers (Table 1) displayed no significant trend with longitude ( $p > 0.05$ ). It should be noted that longitudinal trends with stronger correlations were observed for <sup>13</sup>C PP and BP ( $r = -0.81$  and  $r = -0.82$ , respectively, and  $p < 0.05$ ; Fig. S2 in the Supplement) as well as DIP and NO<sub>3</sub><sup>-</sup> stocks ( $r = -0.68$  and  $r = -0.85$ ,  $p < 0.05$ ; no corre-

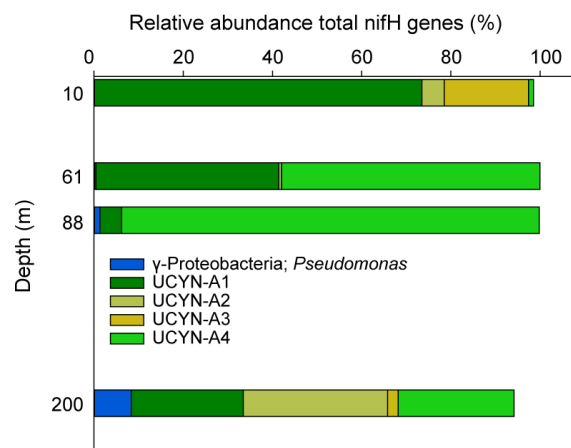


**Figure 4.** Vertical distribution of the 20 most abundant *nifH* ASVs at Station 10, collapsed into major taxonomic groups.

lation with DFe stock; data not shown) integrated over the euphotic layer.

### 3.1.2 N<sub>2</sub> fixation and composition of diazotrophs at Station 10

The westernmost station, Station 10, was in sharp contrast to all other stations, with an euphotic-layer-integrated N<sub>2</sub> fixation on average 44 times higher (Table 1) due to high rates of 2.9 at 37 m and 72.1 nmolNL<sup>-1</sup> d<sup>-1</sup> at 61 m (i.e., at the deep chlorophyll *a* maximum, DCM) (Fig. 2). That rate at 61 m was associated with a maximum in PP but not with a maximum in BP. From the surface to 200 m depth, the *nifH* community composition was largely dominated by ASVs related to different UCYN-A groups (Fig. 4) that represented 86 % at 200 m and up to 99.5 % at the DCM. No UCYN-B and UCYN-C or filamentous diazotrophs were detected. The relative abundance of NCDs (mainly  $\gamma$ -Proteobacteria *Pseudomonas*) increased with depth ( $r = 0.96$ ,  $p < 0.05$ ) to reach about 8 % in the mesopelagic layer (200 m). UCYN-A1 and UCYN-A4 dominated the total diazotrophic community (from 51 % to 99 %). All four UCYN-A had different vertical distributions: the relative abundances of UCYN-A1 and UCYN-A3 were the highest in surface, while UCYN-A4 was dominant at the most productive depths (61 and 88 m). At 61 m depth, where the unusually high rate of N<sub>2</sub> fixation was detected, the community was dominated by both UCYN-A4 (58 %) and UCYN-A1 (41 %).

### 3.1.3 N<sub>2</sub> fixation versus primary production, heterotrophic bacterial production, nutrients

For statistical analysis, due to the high integrated N<sub>2</sub> fixation rate from Station 10, this rate was not included in order to not bias the analysis. N<sub>2</sub> fixation rate integrated over the euphotic layer correlated strongly with PP ( $r = 0.71$ ,  $p < 0.05$ ) and BP ( $r = 0.76$ ,  $p < 0.05$ ) (Fig. 5). Integrated N<sub>2</sub> fixation over

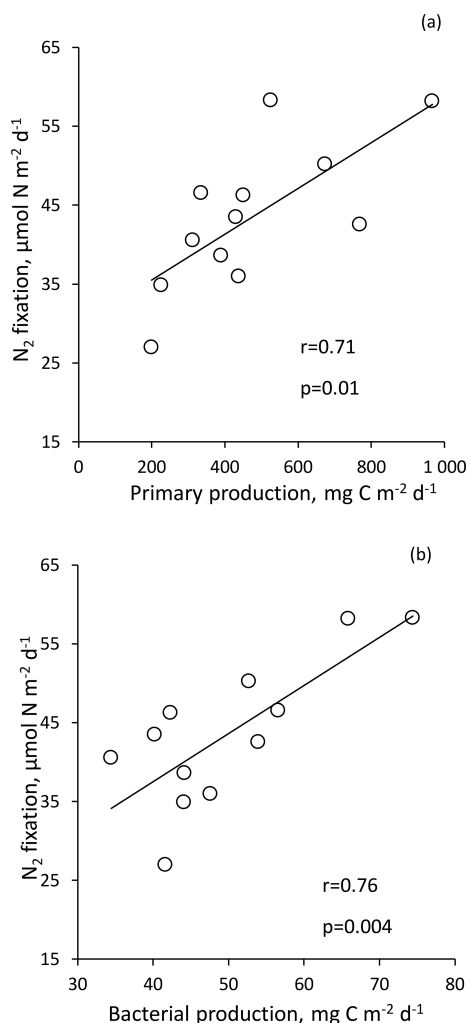


**Figure 5.** N<sub>2</sub> fixation rate integrated over the euphotic layer versus <sup>13</sup>C primary production (a) and bacterial production (b); data at Station 10 were removed.

the euphotic layer (and over the SML) was not correlated with the associated DFe, DIP and NO<sub>3</sub><sup>-</sup> stocks ( $p > 0.05$ ). It should be noted that DIP and NO<sub>3</sub><sup>-</sup> stocks correlated positively with PP and BP ( $p < 0.05$ ) over the euphotic layer (no correlation between DFe stock, PP and BP).

### 3.2 Response of N<sub>2</sub> fixation and composition of the diazotrophic communities to dust seeding

#### 3.2.1 Initial characteristics of the tested seawater

N<sub>2</sub> fixation and BP were the highest at FAST, while PP was the highest at FAST and ION (Table 2). The N<sub>2</sub> fixation rates were similar at ION and TYR and significantly higher (factor ~2.6) at FAST. At TYR and ION, the diazotroph community was largely dominated by NCDs (on average 94.5 % of the total diazotrophic community), whereas at FAST, diazotrophic cyanobacteria, mainly UCYN-A, represented on

average 91.4 % of the total diazotrophic community. NO<sub>3</sub><sup>-</sup> concentration was the highest at FAST (59 nM), while DIP concentration was the highest at TYR (17 nM) and the lowest at ION (7 nM). The molar NO<sub>3</sub><sup>-</sup> : DIP ratio was strongly lower than the Redfield ratio (16 : 1), indicating a potential N limitation of the phytoplanktonic activity in all experiments. DFe concentrations were all higher than 1.5 nM.

#### 3.2.2 Changes in N<sub>2</sub> fixation in response to dust seeding and relationship with changes in primary and heterotrophic bacterial production

All the dust seedings led to a significant stimulation of N<sub>2</sub> fixation relative to the controls under present and future climate conditions (D and G treatments) (Figs. 6 and S3 in the Supplement). The reproducibility between the replicated treatments was good at all stations (mean coefficient of variation (CV, in percent) < 14 %). The maximum N<sub>2</sub> fixation relative change (RC) was the highest at TYR (+434–503 % in D1 and D2, +478–565 % in G1 and G2), then at ION (+256–173 % in D1 and D2 and +261–217 % in G1 and G2) and finally at FAST (+41–49 % in D1 and D2 and +97–120 % in G1 and G2) (Fig. 7). At TYR and FAST, dust addition stimulated N<sub>2</sub> fixation more in the G treatment than in D, whereas at ION the response was similar between the treatments (Fig. S3). N<sub>2</sub> fixation measured during the dust seeding experiments correlated strongly with PP at FAST ( $r = 0.90$ ,  $p < 0.05$ ) and with BP at TYR and ION ( $r > 0.76$ ,  $p < 0.05$ ) (Fig. S4 in the Supplement).

#### 3.2.3 Changes in the diazotrophic composition in response to dust seeding

At TYR and ION, the diazotrophic communities before seeding were largely dominated by NCDs (~94.5 % of total ASVs; Fig. 8, Table 2). These were mainly  $\gamma$ -Proteobacteria related to *Pseudomonas*. Some of these ASVs had low overall relative abundance and therefore did not appear in the top 20 ASVs (Fig. 8, Tables S2 and S3 in the Supplement) but could nevertheless account for up to 16 % in a specific sample. Filamentous cyanobacteria (*Katagnymene*) were also observed at both stations (~4.7 % of the total diazotrophs). The community at FAST was initially dominated by UCYN-A phylotypes, mostly represented by UCYN-A1 and UCYN-A3 (relative abundance of UCYN-A1 and UCYN-A3 in C and D treatments at T0;  $n = 4$ :  $34 \pm 6$  % and  $45 \pm 2$  % of the total diazotrophic composition, respectively; Fig. 8). At TYR and ION, the variability at T0 between replicates was higher than at FAST (Fig. S5 in the Supplement; C1T0 at TYR was removed due to poor sequencing quality). Also, the diversity (Shannon H') was generally higher at TYR and ION at the start of incubations compared to FAST (T0; Fig. S6 in the Supplement). For ION and FAST experiments, *Pseudomonas*-related ASVs were more abundant in G treatments at T0 relative to control and dust treatments (T0). At

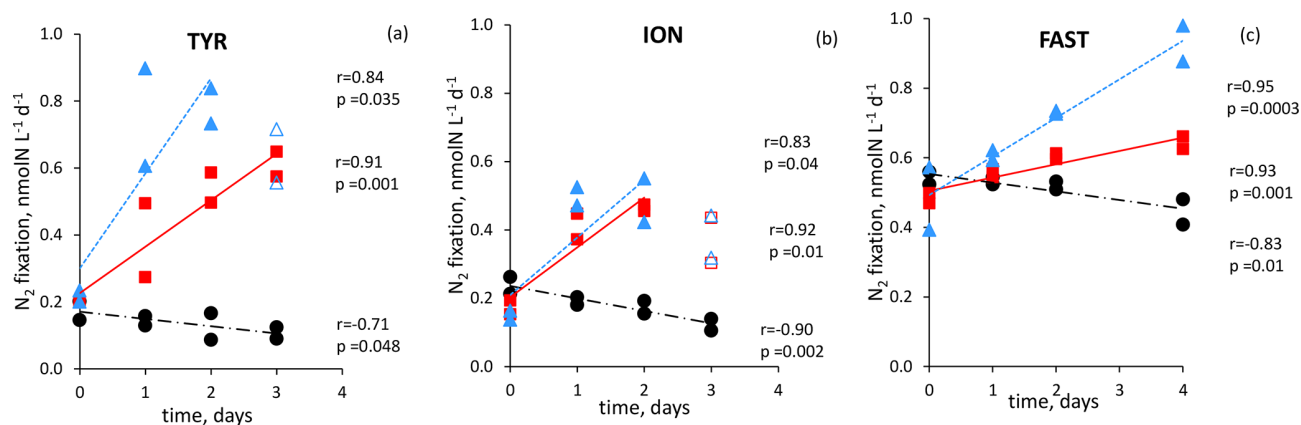


**Figure 6.** N<sub>2</sub> fixation rate in nmol N L<sup>-1</sup> d<sup>-1</sup> during the dust seeding experiments performed at the stations TYR (a), ION (b) and FAST (c) in the replicated controls (black dot), dust treatments under present climate conditions (red square, D treatment) and dust treatments under future climate conditions (blue triangle, G treatments). Open symbols were not included in the linear regression

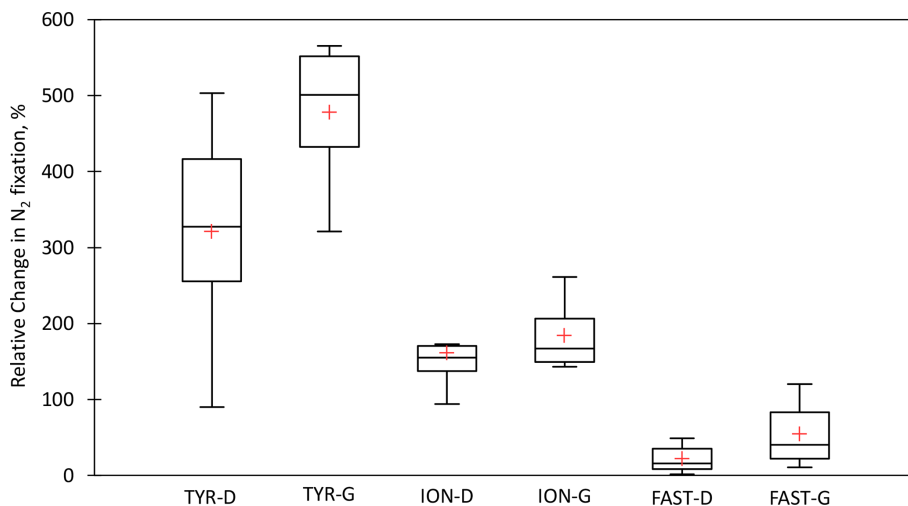


**Figure 7.** Box plots of the relative changes (in percent) in N<sub>2</sub> fixation to the rates measured in the controls over the duration of the dust seeding experiments (T1, T2, and T3 or T4) at TYR, ION and FAST stations. D means dust treatments under present climate conditions (D treatment) and G dust treatments under future climate conditions (G treatment). The red cross represents the average.

the end of the TYR and ION experiments, the community from all treatments appeared to converge (Fig. S5) due to the increase of a few  $\gamma$ -Proteobacteria (mainly *Pseudomonas*) that strongly increased in all treatments (Fig. 8). At FAST, no difference in the relative abundances of diazotrophs was recorded between D treatment and the controls at T4. However, when comparing G treatment relative to D at T4, the relative contribution of NCDs was higher (82 % in G vs. 63 % in D), and the relative abundance of UCYN-A was lower (13 % in G vs. 31 % in D).

#### 4 Discussion

Late spring, at the time of sampling, all the stations were well stratified and characterized by oligotrophic conditions

increasing eastward (Maranon et al., 2021; Fig. 8 in Guieu et al., 2020a). NO<sub>3</sub><sup>-</sup> and DIP concentrations were low in the SML, from 9 to 135 nM for NO<sub>3</sub><sup>-</sup> (Van Wambeke et al., 2021) and from 4 to 17 nM for DIP (Pulido-Villena et al., 2021); the highest stocks were measured at the westernmost station (Station 10) (Table S1).

#### 4.1 General features in N<sub>2</sub> fixation and diazotroph community composition

N<sub>2</sub> fixation rates in the aphotic layer were in the range of those previously measured in the western open MS (Benavides et al., 2016) and accounted, on average, for 41 % of N<sub>2</sub> fixation in the 0–1000 m layer, suggesting that a large part of the total diazotrophic activity was related to heterotrophic NCDs in the aphotic layer. N<sub>2</sub> fixation rates in the euphotic

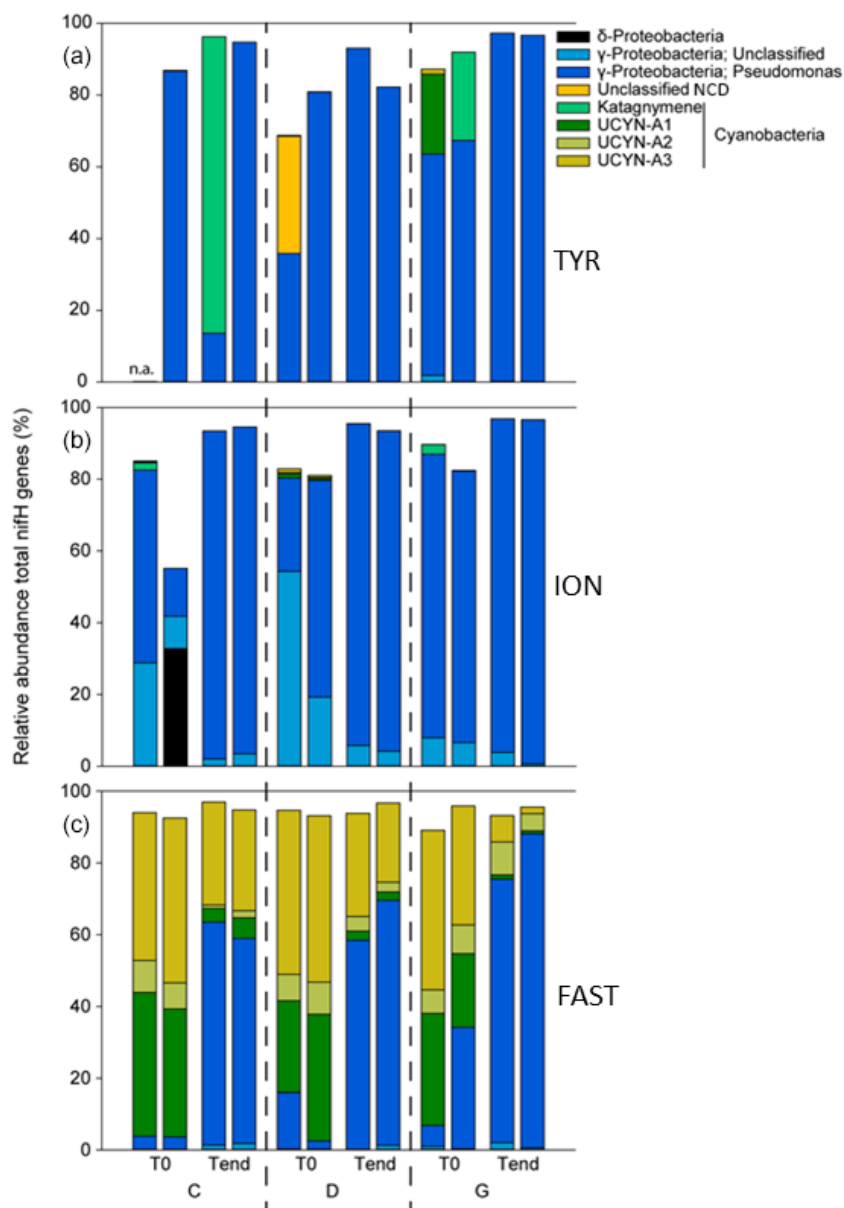


**Figure 8.** The composition of diazotrophs (based on 20 most abundant ASVs in the tanks) during the dust seeding experiments at the start (T0) and end (T3 at TYR and ION and T4 at FAST) in each tank at TYR (a), ION (b) and FAST (c). C1T0 at TYR was not included due to poor sequencing quality.

layer were of the same order of magnitude (data from Station 10 excluded) as those previously measured in the open MS in spring and summer (Bonnet et al., 2011; Rahav et al., 2013). At the tested stations, the surface diazotrophic cyanobacteria were largely dominated by UCYN-A (~93 % of the total diazotrophic cyanobacteria, mostly UCYN-A1 and UCYN-A3) and the NCD community by  $\gamma$ -Proteobacteria (~95 % of the total NCDs). This is the first time that UCYN-A3 and UCYN-A4 are detected in the MS. The photo-autotrophic N<sub>2</sub> fixation was negligible as no UCYN-B and UCYN-C were

detected, and very low abundance of filamentous cyanobacteria was observed.

#### 4.2 Longitudinal gradient of N<sub>2</sub> fixation related to the composition of the diazotrophic communities

At Station 10 and FAST, the surface diazotrophic communities were largely dominated by UCYN-A (> 91 %), whereas at TYR and ION they were dominated by NCDs (> 94 %), which highlights the predominance of photo-heterotrophic diazotrophy in the western waters of the Algerian Basin and of NCD-supported diazotrophy in the Tyrrhenian and Io-

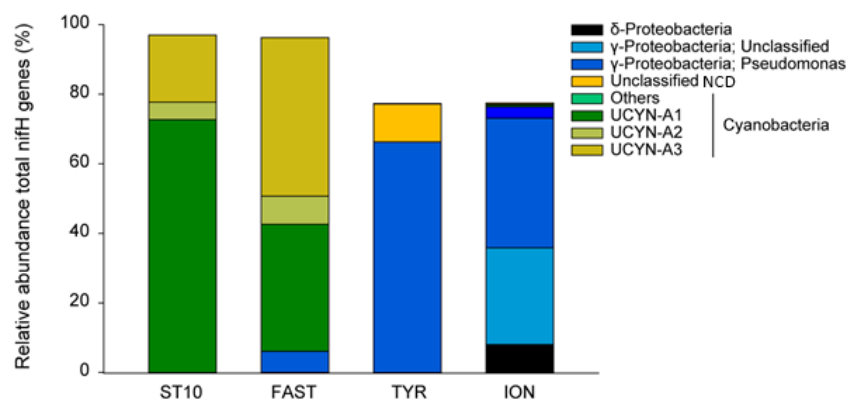


**Figure 9.** Relative abundance of the 20 most abundant *nifH* ASVs in surface waters (values at TYR, ION and FAST are based on average of duplicated control and dust treatments at T0).

nian basins. Surface N<sub>2</sub> fixation exhibited a longitudinal gradient decreasing eastward, as previously reported (Bonnet et al., 2011, Rahav et al., 2013). Strong longitudinal gradients decreasing eastward for the relative abundance of UCYN-A ( $r = -0.93$ ,  $p < 0.05$ ) and inversely increasing eastward for NCDs were observed ( $r = 0.89$ ,  $p < 0.05$ ) (Fig. 9). Despite no quantitative abundances of distinct diazotrophs for the studied area (in this and previously published studies), the intensity of the bulk N<sub>2</sub> fixation rate was likely related to the overall composition of the diazotrophic communities (here relative abundance of UCYN-A versus NCDs). Indeed, surface N<sub>2</sub> fixation rates correlated positively with the relative abundance of UCYN-A (mainly A1 and A3) ( $r = 0.98$ ,  $p < 0.05$ ) and negatively with the relative abundance of NCDs ( $r = -0.99$ ,  $p < 0.05$ ) (Fig. S7 in the Supplement). This could be related, in part, to the variability in the cell-specific N<sub>2</sub> fixation rates that were shown to be higher for UCYN-A relative to NCDs (Turk-Kubo et al., 2014; Bentzon-Tilia et al., 2015; Martinez-Perez et al., 2016; Pearl et al., 2018; Mills et al., 2020). Besides, in Atlantic and Pacific Ocean areas when the diazotrophic community is dominated by unicellular organisms, high N<sub>2</sub> fixation rates are mostly associated with a predominance of UCYN-A and low rates with a predominance of NCDs (Turk-Kubo et al., 2014, Martinez-Perez et al., 2016; Moreiro-Coello et al., 2017, Fonseca-Batista et al., 2019; Tang et al., 2019).

### 4.3 Intriguing Station 10

The patchy distribution of the diazotrophic activity at Station 10 was related to an exceptionally high rate at the DCM ( $72.1 \text{ nmolNL}^{-1} \text{ d}^{-1}$ ). High N<sub>2</sub> fixation rates have previously been observed locally:  $2.4 \text{ nmolNL}^{-1} \text{ d}^{-1}$  at the Strait of Gibraltar (Rahav et al., 2013),  $\sim 5 \text{ nmolNL}^{-1} \text{ d}^{-1}$  in the Bay of Calvi (Rees et al., 2017),  $17 \text{ nmolNL}^{-1} \text{ d}^{-1}$  in the northwestern MS (Garcia et al., 2006) and  $129 \text{ nmolNL}^{-1} \text{ d}^{-1}$  in the eastern MS (Rees et al., 2006). Station 10 was also hydrodynamically “contrasted” com-

pared to the other stations: it was located almost at the center of an anticyclonic eddy (Guiou et al., 2020a), with the core waters (0–200 m) of Atlantic origin (colder, fresher). In such anticyclonic structures, enhanced exchange with nutrient-rich waters from below take place, which, combined with lateral mixing, could explain higher stocks of  $\text{NO}_3^-$  and DIP in the euphotic layer (Table S1). Nevertheless, the anomaly of N<sub>2</sub> fixation at the DCM was associated with anomalies of neither PP, BP nor  $\text{NO}_3^-$  and DIP concentrations. It only coincided with a minimum in DFe concentration ( $0.47 \text{ nM}$  compared to  $0.7$  to  $1.4 \text{ nM}$  at the nearby depths; Bressac et al., 2021). Based on a range of Fe : C (from  $7$  to  $177 \mu\text{mol} : \text{mol}$ ) and associated C : N ratios for diazotrophs (*Trichodesmium*, UCYN) from the literature (Tuit et al., 2004; Berman-Frank et al., 2007; Jiang et al., 2018), we found that  $0.004$  to  $0.08 \text{ nM}$  of DFe is required to sustain this N<sub>2</sub> fixation rate. Consequently, the minimum in DFe concentration at  $61 \text{ m}$  could not be explained solely by the diazotroph uptake.

Despite no correlation between N<sub>2</sub> fixation and the relative abundance of specific diazotrophs ( $p > 0.05$ ) along the profile, the huge heterogeneity in N<sub>2</sub> fixation rate was likely related to the patchy distribution of diazotroph taxa. Indeed, patchiness seems to be a common feature of unicellular diazotrophs (Robidart et al., 2014; Moreira-Coello et al., 2019). The exceptionally high N<sub>2</sub> fixation rates coincided with the highest relative contributions of UCYN-A and more precisely UCYN-A4. Exceptional N<sub>2</sub> fixation rates at Station 10, impacted by northeast Atlantic surface waters of subtropical origin, could thus be related to incoming waters. Indeed, Fonseca-Batista et al. (2019) reported high N<sub>2</sub> fixation rates ( $45$  and  $65 \text{ nmolNL}^{-1} \text{ d}^{-1}$ , with euphotic N<sub>2</sub> fixation rates up to  $1533 \mu\text{molNm}^{-2} \text{ d}^{-1}$ ) associated with a predominance of UCYN-A in subtropical Atlantic surface water mass along the Iberian Margin ( $\sim 40^\circ \text{ N}$ ,  $11^\circ \text{ E}$ ). It should be noted that UCYN-A4 was only detected at Station 10, and its relatively high contribution to the whole diazotrophic community in the euphotic layer coincided with the highest stocks of P (and N) (Table S1). This could reflect higher nutrient requirement(s)

of the UCYN-A4 and/or of its eukaryotic partner relative to other sublineages. Another intriguing feature was the high contribution (~ 86 %) of UCYN-A in the mesopelagic zone (200 m). As UCYN-A lives in obligate symbiosis with haptophytes, from which it receives fixed carbon from photosynthesis (Thompson et al., 2012, 2014), this suggests that this contribution was probably derived from sinking senescing prymnesiophyte UCYN-A cells and that the weak N<sub>2</sub> fixation rate at 200 m depth is likely only driven by  $\gamma$ -Proteobacteria (*Pseudomonas*).

#### 4.4 Supply of bioavailable N from diazotrophic activity for fueling primary and heterotrophic bacterial production – relationship with potential controlling factors of N<sub>2</sub> fixation

The relationship established between N<sub>2</sub> fixation and PP and BP (Fig. 5) illustrated that in the studied area, N<sub>2</sub> fixation is promoted by UCYN and NCDs and/or could indicate that all processes have the same (co)-limitation. Overall, N<sub>2</sub> fixation was a poor contributor to PP ( $1.0 \pm 0.3$  %; Fig. S8 in the Supplement), as previously shown in the MS (Bonnet et al., 2011; Yogev et al., 2011; Rahav et al., 2013) and BP ( $7 \pm 1$  %; Fig. S8), except at Station 10, where N<sub>2</sub> fixation could support up to 19 % of PP (Fig. S8) and supply the entire bioavailable N requirements for heterotrophic prokaryotes (199 % of BP). As expected, our results suggest no control of N<sub>2</sub> fixation by DFe and NO<sub>3</sub><sup>-</sup>, as previously shown through nutrient additions in microcosms (Rees et al., 2006; Ridame et al., 2011, Rahav et al., 2016b). No correlation was observed between N<sub>2</sub> fixation and DIP, which may highlight the spatial variability in the controlling factor of diazotrophs as DIP was shown to control N<sub>2</sub> fixation in the western basin but not in the Ionian Basin (Ridame et al., 2011). Moreover, DIP concentration does not reflect the rapid turnover of P in the open MS and thus could be a poor indicator of DIP availability (Pulido-Villena et al., 2021).

#### 4.5 Diazotrophic activity and composition in response to dust addition under present climate conditions

*General features.* In all experiments, simulated wet dust deposition under present climate conditions triggered a significant (41 to 503 %) and rapid (24–48 h) stimulation of N<sub>2</sub> fixation relative to the controls. Despite this strong increase, N<sub>2</sub> fixation rates remained low ( $< 0.7$  nmol N L<sup>-1</sup> d<sup>-1</sup>) as well as their contribution to PP ( $< 7$  %) and BP ( $< 5$  %), as observed in situ (Sect. 4.4). All of these results are consistent with those found after dust seeding in mesocosms at a coastal site in the northwestern MS (Ridame et al., 2013) and in the open Cretan Sea (Rahav et al., 2016a).

*Temporal changes in the composition of the diazotrophic community.* Dust addition under present climate conditions did not impact the diazotrophic communities' composition. At TYR and ION, the large increase in N<sub>2</sub> fixation recorded

after dust addition might be attributed to NCDs (mainly  $\gamma$ -Proteobacteria), as suggested by the positive correlation between N<sub>2</sub> fixation and BP (Fig. S4). At FAST, the community shifted from a large dominance of UCYN-A towards a dominance of NCDs in both the dust treatments and un-amended controls due to the increase of a few fast growing  $\gamma$ -Proteobacteria (mainly *Pseudomonas*). This shift could be attributed to a bottle effect imposed by the tanks, which can favor fast-growing heterotrophic bacteria (Sherr et al., 1999; Calvo-Diaz et al., 2011). Nevertheless, the increased N<sub>2</sub> fixation after dust seeding at FAST cannot be explained by the shift in composition of the diazotrophic communities because the rates remained quite stable in the controls all along the experiment. Rather, the abundances of diazotrophs have likely increased due to dust input, and UCYN-A in association with prymnesiophytes could still be responsible for the majority of the enhanced N<sub>2</sub> fixation as N<sub>2</sub> fixation correlated strongly with PP (Fig. S4).

*Variability in the N<sub>2</sub> fixation response among stations.* The highest stimulation of N<sub>2</sub> fixation to dust addition was observed at TYR (mean RC<sub>D</sub> = 321 %), then at ION (mean RC<sub>D</sub> = 161 %) and finally at FAST (mean RC<sub>D</sub> = 21 %) (Fig. 7). The differences in the intensity of the diazotrophic response were not related to differences in the initial nutrient stocks (Table S1) and in the nutrient input from dust, which was quite similar between experiments (Gazeau et al., 2021a). Briefly, dust input led to a strong increase of  $11.2 \pm 0.2$   $\mu$ M NO<sub>3</sub><sup>-</sup> a few hours after seeding in the three experiments, and the maximum DIP release was slightly higher at FAST (31 nM) than at TYR and ION ( $23 \pm 2$  nM) (Gazeau et al., 2021a). As DFe concentration before seeding was high ( $\geq 1.5$  nM; Table 2), the bioavailability of Fe did not appear to drive the response of N<sub>2</sub> fixation (Ridame et al., 2013). Also, we evidenced in this experiment that NO<sub>3</sub><sup>-</sup> release from dust did not inhibit N<sub>2</sub> fixation rate driven by UCYN-A and NCDs. This was expected for UCYN-A as it lacks NO<sub>3</sub><sup>-</sup> assimilation pathways (Tripp et al., 2010; Bombar et al., 2014).

N<sub>2</sub> fixation was initially more limited at TYR and ION (as evidenced by the lowest initial rates) compared to FAST, thereby explaining the highest stimulation of N<sub>2</sub> fixation by dust seeding at these stations. Interestingly, the stimulation of N<sub>2</sub> fixation was higher at TYR than at ION (Fig. 7), while these stations presented the same initial rate supported by NCDs. One major difference is that PP was not enhanced by dust seeding at TYR, while BP increased in both experiments (Gazeau et al., 2021b), suggesting that NCD-supported N<sub>2</sub> fixation was not limited by organic carbon at this station. As N<sub>2</sub> fixation and BP correlated strongly after the dust seeding (Fig. S4), it means that dust-derived DIP could relieve the ambient limitation of both heterotrophic prokaryotes (BP was co-limited by NP; Van Wambeke et al., 2021) and NCDs at TYR. This could explain why DIP concentration in the D treatments became again similar to the controls at the end of this experiment (Gazeau et al., 2021a). At ION, characterized by the lowest initial DIP concentration, N<sub>2</sub> fixation

and PP were likely DIP (co-)limited as shown for BP (Van Wambeke et al., 2021). Consequently, diazotrophs as well as non-diazotrophs (heterotrophic prokaryotes and photoautotrophs) could all take up the dust-derived DIP, reducing then potentially the amount of DIP available for each cell that could explain the lower stimulation of N<sub>2</sub> fixation relative to TYR.

At FAST, initially dominated by UCYN-A, N<sub>2</sub> fixation and PP correlated strongly after the dust seeding (Fig. S4c). This indicated that dust could relieve either directly the ambient nutrient limitation of both N<sub>2</sub> fixation and PP (Fig. S9 in the Supplement) or indirectly through first the relief of the PP limitation of the UCYN-A photoautotroph hosts, inducing an increase in the production of organic carbon, which could be used by UCYN-A to increase its N<sub>2</sub>-fixing activity. Nutrients from dust could also first enhance the UCYN-A-supported N<sub>2</sub> fixation, which in turn could relieve the N limitation of the UCYN-A photoautotrophic host as the initial NO<sub>3</sub><sup>-</sup> : DIP ratio indicates a potential N limitation of the PP (Table 2).

#### 4.6 Response to dust addition under future relative to present climate conditions

*General features.* At TYR and FAST, N<sub>2</sub> fixation was more stimulated by dust input under future than present climate conditions (mean RC<sub>G-TYR</sub> = 478 % and mean RC<sub>G-FAST</sub> = 54 %), whereas at ION the response was similar (Figs. 7 and S3). These differences between future and present climate conditions were not related to the nutrients supplied from dust (Gazeau et al., 2021a).

The purpose of our study was to study the combined effect of warming and acidification, but we can expect on the short timescale of our experiments (< 3–4 d) that NCDs and UCYN-A would not be directly affected by the changes in the CO<sub>2</sub> concentration as they do not fix CO<sub>2</sub> (Zehr et al., 2008). Indeed, no impact of acidification (or increase in the partial pressure of CO<sub>2</sub>) on N<sub>2</sub> fixation was detected when the diazotrophic communities were dominated by UCYN-A in the North and South Pacific (Law et al., 2012; Böttjer et al., 2014). Nevertheless, the decrease in pH may indirectly impact UCYN-A through changes affecting its autotrophic host.

*TYR and ION.* Under future climate conditions, the composition of the diazotrophic communities did not change after dust input at TYR and ION relative to present conditions. At TYR, the highest N<sub>2</sub> fixation stimulation might be linked to the increase in the NCD abundances and/or in their cell-specific N<sub>2</sub> fixation rates under future climate conditions. Unfortunately, the impact of increased temperature and decreased pH on the cell-specific N<sub>2</sub> fixation rates of NCDs is currently unknown. However, some studies suggest a positive relationship between temperature and abundances of NCDs: diazotrophic  $\gamma$ -Proteobacteria ( $\gamma$ -24774A11) gene copies correlated positively with temperature (from ~20 to 30 °C) in surface waters of the western South Pacific Ocean

(Moisander et al., 2014), and Messer et al. (2015) suggested a temperature optimum for these  $\gamma$ -Proteobacteria around 25–26 °C in the Australian tropical waters. At ION, the similar stimulation of N<sub>2</sub> fixation by dust under future climate conditions compared to present climate conditions could be explained by a greater mortality of diazotrophs due to a higher grazing pressure and/or a higher viral activity. Indeed, higher bacterial mortality in the G treatment that could be related to a higher grazing pressure has been observed (Dinasquet et al., 2021). Another explanation is that in spite of the DIP supply from the dust, the DIP bioavailability, initially the lowest at ION, was not sufficient to allow an additional N<sub>2</sub> fixation stimulation.

*FAST.* Some differences in the composition of the diazotrophic communities were observed between present and future climate conditions at FAST after dust input: the contribution of NCDs (mainly *Pseudomonas*) increased, and that of UCYN-A decreased. It must be noted that the duration of the experiment was longer at FAST (4 d) relative to TYR and ION (3 d), which could explain at least partly differences between stations. A direct response of increased temperature and/or decreased pH can be considered on a very short timescale (12 h) by comparing the results in the G treatment at T0 (+3 °C, –0.3 pH unit) with those in C and D treatments. The increased contribution of *Pseudomonas* in the G treatment at T0 (before dust addition) reveals a likely positive effect of temperature on the growth of this NCD as an increase in the top-down control on the bacterioplankton was observed after dust seeding under future climate conditions (Dinasquet et al., 2021). Interestingly, despite the decrease in the relative contribution of UCYN-A to the total diazotroph community after dust addition, we observed contrasted responses within the UCYN-A group relative to present climate conditions: the relative abundance of UCYN-A3 strongly decreased (4.6 % in G vs. 25.4 % in D), whereas the relative abundance of UCYN-A2 was twice as high (7 % in G vs. 3.4 % in D). Notably, the relative contribution of UCYN-A1 did not appear to be impacted during the dust addition experiment. These respective changes could be explained by the difference in the temperature tolerance between UCYN-A2 and UCYN-A3. Temperature is one of the key drivers explaining the distribution of UCYN-A, which appeared to dominate in most of the temperate regions, with temperature optima around ~20–24 °C (Langlois et al., 2008; Moisander et al., 2010). However, the temperature optima for the different UCYN-A sublineages, in particular for UCYN-A2 and UCYN-A3, are poorly known. Interestingly, Henke et al. (2018) observed that the absolute UCYN-A2 abundance was positively affected by increasing temperature, within a range of temperature from about 21 to 28 °C, which is in agreement with our results, although only relative abundances were measured in our study. Based on the strong positive correlation between N<sub>2</sub> fixation and PP after dust addition (and no correlation between N<sub>2</sub> fixation and BP; Fig. S4) and despite the decrease in the relative abun-



dance of UCYN-A3, the increased stimulation of N<sub>2</sub> fixation under future climate conditions could likely be sustained by the increase in the relative abundance of UCYN-A2, which is bigger than UCYN-A3 (Cornejo-Castillo et al., 2019) and could consequently have a higher cell-specific N<sub>2</sub> fixation rate.

## 5 Conclusions

In the MS, N<sub>2</sub> fixation is a minor pathway to supply new bioavailable N for sustaining both PP and BP but can locally support up to 20% of PP and provide all the N requirements for bacterial activity. UCYN-A might be supporting extremely high rates of N<sub>2</sub> fixation (72 nmol L<sup>-1</sup> d<sup>-1</sup>) in the core of an eddy in the Algerian Basin influenced by Atlantic waters. The eastward-decreasing longitudinal trend of N<sub>2</sub> fixation in the surface waters is likely related to the spatial variability in the composition of the diazotrophic communities, as shown by the eastward increase in the relative abundance of NCDs towards more oligotrophic waters, while we observed a westward increase in the relative abundance of UCYN-A. This could reflect lower nutrient requirements for NCDs relative to UCYN-A. Through the release of new nutrients, simulated wet dust deposition under present and future climate conditions significantly stimulated N<sub>2</sub> fixation. The degree of stimulation depended on the metabolic activity of the diazotrophs (degree of limitation) related to the composition of diazotrophic communities and on the ambient potential nutrient limitations of diazotrophs, including that of the UCYN-A prymnesiophyte host. The strongest increase in N<sub>2</sub> fixation, not accompanied with a change in the composition of the diazotrophic communities, was observed at the stations dominated by NCDs (TYR, ION), where the nutrient limitation was the strongest. Under projected future levels of temperature and pH, the dust effect is either exacerbated or unchanged. Knowing that NCDs and UCYN-A do not fix CO<sub>2</sub>, we suggest that, on the timescale of our experiments (3–4 d), the exacerbated response of N<sub>2</sub> fixation is likely the result of the warming (from about 21 to 24 °C), which may increase the growth of NCDs when nutrient availability allows it and may alter the composition of UCYN-A community. However, to date, the effect of acidification and temperature optima of the different UCYN-A sublineages is poorly known (or unknown) as these UCYN-A remain uncultivated.

Future changes in climate, desertification and land use practices could induce an increase in dust deposition to the oceans (Tegen et al., 2004; Moulin and Chiapello, 2006; Klingmüller et al., 2016). The predicted future increase in surface temperature and the resulting stronger stratification are expected to expand the surface of low-nutrient, low-chlorophyll (LNLC) areas, consequently reinforcing the role of new nutrient supply from eolian dust on the N<sub>2</sub> fixation and probably on the structure of the diazotrophic communities.

*Data availability.* The PEACETIME dataset will be available at <https://doi.org/10.17882/75747> (Guieu et al., 2020b) upon publication of all papers in the special issue (January 2022).

*Supplement.* The supplement related to this article is available online at: <https://doi.org/10.5194/bg-19-415-2022-supplement>.

*Author contributions.* FG and CG designed the dust seedings experiments. CR, JD, EB, MB, FVW, FG, VT, ATS and CG participated in the sampling and analysis. CR and EB performed DNA extraction; EB performed library preparation. CR, JD and SH analyzed the data; CR wrote the manuscript with contributions from all authors.

*Competing interests.* The contact author has declared that neither they nor their co-authors have any competing interests.

*Disclaimer.* Publisher's note: Copernicus Publications remains neutral with regard to jurisdictional claims in published maps and institutional affiliations.

*Special issue statement.* This article is part of the special issue “Atmospheric deposition in the low-nutrient–low-chlorophyll (LNLC) ocean: effects on marine life today and in the future (ACP/BG inter-journal SI)”. It is not associated with a conference.

*Acknowledgement.* The authors thank the captain and the crew of the RV *Pourquoi Pas?* for their professionalism and their work at sea. We warmly acknowledge our second chief scientist Karine Desboeufs. We gratefully thank Eric Thiebaut and Pierre Kostyrka for their precious advice with statistical tests. We also thank Kahina Djaoudi and Thibaut Wagener for their assistance in sampling the tanks and TMC rosette and Magloire Mandeng-Yogo and Fethiye Cetin for IRMS measurements at the Alyses platform (SU, IRD). The DIC data used in this study were analyzed at the SNAP-CO<sub>2</sub> service facility at the LOCEAN laboratory and supported by the CNRS-INSU and OSU Ecce-Terra. We greatly appreciate the interest of the reviewers and Christine Klaas and thank them for their relevant comments and time spent reviewing our manuscript.

*Financial support.* This study is a contribution to the PEACETIME project (<http://peacetime-project.org>, last access: 17 January 2022), a joint initiative of the MERMEX and ChArMEX components supported by the CNRS-INSU, IFREMER, CEA and Météo-France as part of the program MISTRALS coordinated by the INSU. PEACETIME was endorsed as a process study by GEOTRACES. Julie Dinasquet was funded by a Marie Curie Actions International Outgoing Fellowship (PIOF-GA-2013-629378). Søren Hallstrøm and Lasse Riemann were funded by grant 6108-00013 from the Danish Council for Independent Research.

*Review statement.* This paper was edited by Carolin Löscher and reviewed by two anonymous referees.

## References

- Aminot, A. and K erouel, R.: Dosage automatique des nutriments dans les eaux marines, in: M ethodes d'analyses en milieu marin, edited by: edited by: IFREMER, Editions Quae, Versailles, 188 pp., 2007.
- Angel, R., Nepel, M., Panh ozl, C., Schmidt, H., Herbold, C. W., Eichorst, S. A., and Woebken, D.: Evaluation of primers targeting the diazotroph functional gene and development of NifMAP-A bioinformatics pipeline for analyzing nifH amplicon data, *Front. Microbiol.*, 9, 703, <https://doi.org/10.3389/fmicb.2018.00703>, 2018.
- Bar Zeev, E., Yogev, T., Man-Aharonovich, D., Kress, N., Herut, B., Beja, O., and Berman-Frank, I.: Seasonal dynamics of the endosymbiotic, nitrogen-fixing cyanobacterium *Richelia intracellularis* in the Eastern Mediterranean Sea, *ISME J.*, 2, 911–923, <https://doi.org/10.1038/ismej.2008.56>, 2008.
- Benavides, M., Bonnet, S., Hern andez, N., Mart inez-P erez, A. M., Nieto-Cid, M., and  lvarez-Salgado, X. A.: Basin-wide N<sub>2</sub> fixation in the deep waters of the Mediterranean Sea, *Global Biogeochem. Cy.*, 30, 952–961, <https://doi.org/10.1002/2015GB005326>, 2016.
- Bentzon-Tilia, M., Traving, S. J., Mantikci, M., Knudsen-Leerbeck, H., Hansen, J. L. S., Markager, S., and Riemann, L.: Significant N<sub>2</sub> fixation by heterotrophs, photoheterotrophs and heterocystous cyanobacteria in two temperate estuaries, *ISME J.*, 9, 273–285, <https://doi.org/10.1038/ismej.2014.119>, 2015.
- Berman-Frank, I. A., Quigg, A., Finkel, Z. V., Irwin, A. J., and Haramaty, L.: Nitrogen-fixation strategies and Fe requirements in cyanobacteria, *Limnol. Oceanogr.*, 52, 2260–2269, 2007.
- Bigear, E., Lopes Dos Santos, A., and Ribeiro, C.: nifH amplification for Illumina sequencing, [protocols.io](https://doi.org/10.17504/protocols.io.bkipkudn), <https://doi.org/10.17504/protocols.io.bkipkudn>, 2021.
- Bonnet, S. and Guieu, C.: Atmospheric forcing on the annual in the Mediterranean Sea. A one year survey, *J. Geophys. Res.*, 111, C09010, <https://doi.org/10.1029/2005JC003213>, 2006.
- Bonnet, S., Grosso, O., and Moutin, T.: Planktonic dinitrogen fixation along a longitudinal gradient across the Mediterranean Sea during the stratified period (BOUM cruise), *Biogeosciences*, 8, 2257–2267, <https://doi.org/10.5194/bg-8-2257-2011>, 2011.
- Bosc, E., Bricaud, A., and Antoine, D.: Seasonal and inter-annual variability in algal biomass and primary production in the Mediterranean Sea, as derived from 4 years of SeaWiFS observations, *Global Biogeochem. Cy.*, 18, GB1005, <https://doi.org/10.1029/2003GB002034>, 2004.
- Bolyen, E., Rideout, J. R., Dillon, M. R., Bokulich, N. A., Abnet, C. C., Al-Ghalith, G. A., Alexander, H., Alm, E. J., Arumugam, M., Asnicar, F., Bai, Y., Bisanz, J. E., Bittinger, K., Brejnrod, A., Brislawn, C. J., Brown, C. T., Callahan, B. J., Caraballo-Rodr guez, A. M., Chase, J., Cope, E. K., Da Silva, R., Diener, C., Dorrestein, P. C., Douglas, G. M., Durall, D. M., Duvall, C., Edwardson, C. F., Ernst, M., Estaki, M., Fouquier, J., Gauglitz, J. M., Gibbons, S. M., Gibson, D. L., Gonzalez, A., Gorlick, K., Guo, J., Hillmann, B., Holmes, S., Holste, H., Huttenhower, C., Huttley, G. A., Janssen, S., Jarmusch, A. K., Jiang, L., Kaehler, B. D., Kang, K. B., Keefe, C. R., Keim, P., Kelley, S. T., Knights, D., Koester, I., Kosci lek, T., Kreps, J., Langille, M. G. I., Lee, J., Ley, R., Liu, Y. X., Lofthfield, E., Lozupone, C., Maher, M., Marotz, C., Martin, B. D., McDonald, D., McIver, L. J., Melnik, A. V., Metcalf, J. L., Morgan, S. C., Morton, J. T., Naimey, A. T., Navas-Molina, J. A., Nothias, L. F., Orchanian, S. B., Pearson, T., Peoples, S. L., Petras, D., Preuss, M. L., Pruesse, E., Rasmussen, L. B., Rivers, A., Robeson, M. S., Rosenthal, P., Segata, N., Shaffer, M., Shiffer, A., Sinha, R., Song, S. J., Spear, J. R., Swafford, A. D., Thompson, L. R., Torres, P. J., Trinh, P., Tripathi, A., Turnbaugh, P. J., Ul-Hasan, S., van der Hooft, J. J. J., Vargas, F., V azquez-Baeza, Y., Vogtmann, E., von Hippel, M., Walters, W., Wan, Y., Wang, M., Warren, J., Weber, K. C., Williamson, C. H. D., Willis, A. D., Xu, Z. Z., Zaneveld, J. R., Zhang, Y., Zhu, Q., Knight, R., and Caporaso, J. G.: Reproducible, interactive, scalable and extensible microbiome data science using QIIME 2, *Nat. Biotechnol.*, 37, 852–857, <https://doi.org/10.1038/s41587-019-0209-9>, 2019.
- Bombar, D., Heller, P., Sanchez-Baracaldo, P., Carter, B. J., and Zehr, J. P.: Comparative genomics reveals surprising divergence of two closely related strains of uncultivated UCYN-A cyanobacteria, *ISME J.*, 8, 2530–2542, <https://doi.org/10.1038/ismej.2014.167>, 2014.
- B ttjer, D., Karl, D. M., Letelier, R. M., Viviani, D. A., and Church, M. J.: Experimental assessment of diazotroph responses to elevated seawater pCO<sub>2</sub> in the North Pacific Subtropical Gyre, *Global Biogeochem. Cy.*, 28, 601–616, <https://doi.org/10.1002/2013GB004690>, 2014.
- Bressac, M., Wagener, T., Leblond, N., Tovar-S nchez, A., Ridame, C., Taillandier, V., Albani, S., Guasco, S., Dufour, A., Jacquet, S. H. M., Dulac, F., Desboeufs, K., and Guieu, C.: Subsurface iron accumulation and rapid aluminum removal in the Mediterranean following African dust deposition, *Biogeosciences*, 18, 6435–6453, <https://doi.org/10.5194/bg-18-6435-2021>, 2021.
- Buchfink, B., Xie, C., and Huson, D. H.: Fast and sensitive protein alignment using DIAMOND, *Nat. Methods*, 12, 1, 59–60, <https://doi.org/10.1038/nmeth.3176>, 2015.
- Callahan, B. J., Mc Murdie, P. J., Rosen, M. J., Han, A. W., Johnson, A. J. A., and Holmes, S.: DADA2: High-resolution sample inference from Illumina amplicon data, *Nat. Methods*, 13, 581, <https://doi.org/10.1038/nmeth.3869>, 2016.
- Calvo-D az, A., D az-P erez, L., Su arez, L.  ., Mor n, X. A. G., Teira, E., and Mara n n, E.: Decrease in the autotrophic-to-heterotrophic biomass ratio of picoplankton in oligotrophic marine waters due to bottle enclosure, *Appl. Environ. Microbiol.*, 77, 5739–5746, <https://doi.org/10.1128/AEM.00066-11>, 2011.
- Clarke, K. R. and Warwick, P. E.: Change in Marine Communities: An Approach to Statistical Analysis and Interpretation, Primer-E Ltd, Plymouth, UK, 2001.
- Cornejo-Castillo, F. M., Munoz-Marin, M. D. C., Turk-Kubo, K. A., Royo-Llonch, M., Farnelid, H., Acinas, S. G., and Zehr, J. P.: UCYN-A3, a newly characterized open ocean sublineage of the symbiotic N<sub>2</sub>-fixing cyanobacterium *Candidatus Ateolycyanobacterium Thalassa*, *Environ. Microbiol.*, 21, 111–124, <https://doi.org/10.1111/1462-2920.14429>, 2019.
- Desboeufs, K. V., Losno, R., and Colin, J.-L.: Factors influencing aerosol solubility during cloud processes, *Atmos. Environ.*, 35, 3529–3537, [https://doi.org/10.1016/S1352-2310\(00\)00472-6](https://doi.org/10.1016/S1352-2310(00)00472-6), 2001.

- Desboeufs, K., Leblond, N., Wagener, T., Bon Nguyen, E., and Guieu, C.: Chemical fate and settling of mineral dust in surface seawater after atmospheric deposition observed from dust seeding experiments in large mesocosms, *Biogeosciences*, 11, 5581–5594, <https://doi.org/10.5194/bg-11-5581-2014>, 2014.
- Dinasquet, J., Bigeard, E., Gazeau, F., Azam, F., Guieu, C., Marañón, E., Ridame, C., Van Wambeke, F., Obernosterer, I., and Baudoux, A.-C.: Impact of dust addition on the microbial food web under present and future conditions of pH and temperature, *Biogeosciences Discuss.* [preprint], <https://doi.org/10.5194/bg-2021-143>, in review, 2021.
- D'Ortenzio, F. and Ribera d'Alcalà, M.: On the trophic regimes of the Mediterranean Sea: a satellite analysis, *Biogeosciences*, 6, 139–148, <https://doi.org/10.5194/bg-6-139-2009>, 2009.
- D'Ortenzio, F., Iudicone, D., de Boyer Montegut, C., Testor, P., Antoine, D., Marullo, S., Santoleri, R., and Madec, G.: Seasonal variability of the mixed layer depth in the Mediterranean Sea as derived from in situ profiles, *Geophys. Res. Lett.*, 32, L12605, <https://doi.org/10.1029/2005GL022463>, 2005.
- Eichner, M., Rost, B., and Kranz, S.: Diversity of ocean acidification effects on marine N<sub>2</sub> fixers, *J. Exp. Mar. Biol. Ecol.*, 457, 199–207, <https://doi.org/10.1016/j.jembe.2014.04.015>, 2014.
- El Hourany, R., Abboud-Abi Saab, M., Faour, G., Mejia, C., Crépon, M., and Thiria, S.: Phytoplankton diversity in the Mediterranean Sea from satellite data using self-organizing maps, *J. Geophys. Res.-Oceans*, 124, 5827–5843, <https://doi.org/10.1029/2019JC015131>, 2019.
- Farnelid, H., Turk-Kubo, K. A., del Carmen Muñoz-Marín, M., and Zehr, J. P.: New insights into the ecology of the globally significant uncultured nitrogen-fixing symbiont UCYN-A, *Aquat. Microb. Ecol.*, 77, 125–138, <https://doi.org/10.3354/ame01794>, 2016.
- Fonseca-Batista, D., Li, X., Riou, V., Michotey, V., Deman, F., Fripiat, F., Guasco, S., Brion, N., Lemaitre, N., Tonnard, M., Gallinari, M., Planquette, H., Planchon, F., Sarthou, G., Elskens, M., LaRoche, J., Chou, L., and Dehairs, F.: Evidence of high N<sub>2</sub> fixation rates in the temperate northeast Atlantic, *Biogeosciences*, 16, 999–1017, <https://doi.org/10.5194/bg-16-999-2019>, 2019.
- Frank, I. E., Turk-Kubo, K. A., and Zehr, J. P.: Rapid annotation of nif H gene sequences using classification and regression trees facilitates environmental functional gene analysis, *Env. Microbiol. Rep.*, 8, 905–916, <https://doi.org/10.1111/1758-2229.12455>, 2016.
- Fu, F.-X., Mulholland, M. R., Garcia, N. S., Beck, A., Bernhardt, P. W., Warner, M. E., Sanudo-Wilhelmy, S. A., and Hutchins, D. A.: Interactions between changing pCO<sub>2</sub>, N<sub>2</sub> fixation, and Fe limitation in the marine unicellular cyanobacterium *Crocospaera*, *Limnol. Oceanogr.*, 53, 2472–2484, <https://doi.org/10.4319/llo.2008.53.6.2472>, 2008.
- Fu, F.-X., Yu, E., Garcia, N. S., Gale, Y., Luo, Y., Webb, E. A., and Hutchins, D. A.: Differing responses of marine N<sub>2</sub> fixers to warming and consequences for future diazotroph community structure, *Aquat. Microb. Ecol.*, 72, 33–46, <https://doi.org/10.3354/ame01683>, 2014.
- Fukuda, R., Ogawa, H., Nagata, T., and Koike, I.: Direct determination of carbon and nitrogen contents of natural bacterial assemblages in marine environments, *Appl. Environ. Microb.*, 64, 3352–3358, <https://doi.org/10.1128/aem.64.9.3352-3358.1998>, 1998.
- Garcia, N., Raimbault, P., Gouze, E., and Sandroni, V.: Nitrogen fixation and primary production in Western Mediterranean, *C. R. Biol.*, 329, 742–750, <https://doi.org/10.1016/j.crvi.2006.06.006>, 2006.
- Gazeau, F., Ridame, C., Van Wambeke, F., Alliouane, S., Stolpe, C., Irisson, J.-O., Marro, S., Grisoni, J.-M., De Liège, G., Nunige, S., Djaoudi, K., Pulido-Villena, E., Dinasquet, J., Obernosterer, I., Catala, P., and Guieu, C.: Impact of dust addition on Mediterranean plankton communities under present and future conditions of pH and temperature: an experimental overview, *Biogeosciences*, 18, 5011–5034, <https://doi.org/10.5194/bg-18-5011-2021>, 2021a.
- Gazeau, F., Van Wambeke, F., Marañón, E., Pérez-Lorenzo, M., Alliouane, S., Stolpe, C., Blasco, T., Leblond, N., Zäncker, B., Engel, A., Marie, B., Dinasquet, J., and Guieu, C.: Impact of dust addition on the metabolism of Mediterranean plankton communities and carbon export under present and future conditions of pH and temperature, *Biogeosciences*, 18, 5423–5446, <https://doi.org/10.5194/bg-18-5423-2021>, 2021b.
- Giorgi, F.: Climate change Hot-spots, *Geophys. Res. Lett.*, 33, L08707, <https://doi.org/10.1029/2006GL025734>, 2006.
- Guieu, C. and Ridame, C.: Impact of atmospheric deposition on marine chemistry and biogeochemistry, in: *Atmospheric Chemistry in the Mediterranean Region: Comprehensive Diagnosis and Impacts*, edited by: Dulac, F., Sauvage, S., and Hamonou, E., Springer, Cham, Switzerland, 2020.
- Guieu, C., Dulac, F., Desboeufs, K., Wagener, T., Pulido-Villena, E., Grisoni, J.-M., Louis, F., Ridame, C., Blain, S., Brunet, C., Bon Nguyen, E., Tran, S., Labiadh, M., and Dominici, J.-M.: Large clean mesocosms and simulated dust deposition: a new methodology to investigate responses of marine oligotrophic ecosystems to atmospheric inputs, *Biogeosciences*, 7, 2765–2784, <https://doi.org/10.5194/bg-7-2765-2010>, 2010.
- Guieu, C., D'Ortenzio, F., Dulac, F., Taillandier, V., Doglioli, A., Petrenko, A., Barrillon, S., Mallet, M., Nabat, P., and Desboeufs, K.: Introduction: Process studies at the air–sea interface after atmospheric deposition in the Mediterranean Sea – objectives and strategy of the PEACETIME oceanographic campaign (May–June 2017), *Biogeosciences*, 17, 5563–5585, <https://doi.org/10.5194/bg-17-5563-2020>, 2020a.
- Guieu, C., Desboeufs, K., Albani, S., Alliouane, S., Aumont, O., Barbieux, M., Barrillon, S., Baudoux, A.-C., Berline, L., Bhairy, N., Bigeard, E., Bloss, M., Bressac, M., Brito, J., Carlotti, F., de Liege, G., Dinasquet, J., Djaoudi, K., Doglioli, A., D'Ortenzio, F., Doussin, J.-F., Duforet, L., Dulac, F., Dutay, J.-C., Engel, A., Feliu-Brito, G., Ferre, H., Formenti, P., Fu, F., Garcia, D., Garel, M., Gazeau, F., Giorio, C., Gregori, G., Grisoni, J.-M., Guasco, S., Guittonneau, J., Haëntjens, N., Heimbürger, L.-E., Helias, S., Jacquet, S., Laurent, B., Leblond, N., Lefevre, D., Mallet, M., Marañón, E., Nabat, P., Nicosia, A., Obernosterer, I., Perez, L. M., Petrenko, A., Pulido-Villena, E., Raimbault, P., Ridame, C., Riffault, V., Rougier, G., Rousselet, L., Roy-Barman, M., Saiz-Lopez, A., Schmechtig, C., Sellegri, K., Siour, G., Taillandier, V., Tamburini, C., Thyssen, M., Tovar-Sanchez, A., Triquet, S., Uitz, J., Van Wambeke, F., Wagener, T., and Zaencker, B.: BIOGEO-CHEMICAL dataset collected during the PEACETIME cruise, SEANOIE [data set], <https://doi.org/10.17882/75747>, 2020b.
- Hama, T., Miyazaki, T., Ogawa, Y., Iwakuma, T., Takahashi, M., Otsuki, A., and Ichimura, S.: Measurement of pho-

- tosynthetic production of a marine phytoplankton population using a stable <sup>13</sup>C isotope, *Mar. Biol.*, 73, 31–36, <https://doi.org/10.1007/BF00396282>, 1983.
- Henke, B. A., Turk-Kubo, K. A., Bonnet, S., and Zehr, J. P.: Distributions and Abundances of Sublineages of the N<sub>2</sub>-Fixing Cyanobacterium *Candidatus Atelocyanobacterium thalassa* (UCYN-A) in the New Caledonian Coral Lagoon, *Front. Microbiol.*, 9, 554, <https://doi.org/10.3389/fmicb.2018.00554>, 2018.
- Herut, B., Zohary, T., Krom, M. D., Mantoura, R. F., Pitta, P., Psarra, S., Rassoulzadegan, F., Tanaka, T., and Thingstad, T. F.: Response of East Mediterranean surface water to Saharan dust: On-board microcosm experiment and field observations, *Deep-Sea Res. Pt. II*, 52, 3024–3040, <https://doi.org/10.1016/j.dsr2.2005.09.003>, 2005.
- Herut, B., Rahav, E., Tsagaraki, T. M., Giannakourou, A., Tsiola, A., Psarra, S., Lagaria, A., Papageorgiou, N., Mihalopoulos, N., Theodosi, C. N., Violaki, K., Stathopoulou, E., Scoulios, M., Krom, M. D., Stockdale, A., Shi, Z., Berman-Frank, I., Meador, T. B., Tanaka, T., and Paraskevi, P.: The potential impact of Saharan dust and polluted aerosols on microbial populations in the East Mediterranean Sea, an overview of a mesocosm experimental approach, *Front. Mar. Sci.*, 3, 226, <https://doi.org/10.3389/fmars.2016.00226>, 2016.
- Hutchins, D., Fu, F.-X., Webb, E., Walworth, N., and Tagliabue, A.: Taxon-specific response of marine nitrogen fixers to elevated carbon dioxide concentrations, *Nat. Geosci.*, 6, 790–795, <https://doi.org/10.1038/ngeo1858>, 2013.
- Ibello, V., Cantoni, C., Cozzi, S., and Civitarese, G.: First basin-wide experimental results on N<sub>2</sub> fixation in the open Mediterranean Sea, *Geophys. Res. Lett.*, 37, L03608, <https://doi.org/10.1029/2009GL041635>, 2010.
- Ignatiades, L., Gotsis-Skretas, O., Pagou, K., and Krasakopoulou, E.: Diversification of phytoplankton community structure and related parameters along a large-scale longitudinal east-west transect of the Mediterranean Sea, *J. Plankton. Res.*, 31, 411–428, <https://doi.org/10.1093/plankt/fbn124>, 2009.
- IPCC: IPCC Special Report on the Ocean and Cryosphere in a Changing Climate, edited by: Pörtner, H.-O., Roberts, D. C., Masson-Delmotte, V., Zhai, P., Tignor, M., Poloczanska, E., Mintenbeck, K., Alegría, A., Nicolai, M., Okem, A., Petzold, J., Rama, B., and Weyer, N. M., in press, 2019.
- Jiang, H. B., Fu, F.-X., Rivero-Calle, S., Levine, N. M., Sañudo-Wilhelmy, S. A., Qu, P. P., Wang, X. W., Pinedo-Gonzalez, P., Zhu, Z., and Hutchins, D. A.: Ocean warming alleviates iron limitation of marine nitrogen fixation, *Nat. Clim. Change*, 8, 709–712, <https://doi.org/10.1038/s41558-018-0216-8>, 2018.
- Klingmüller, K., Pozzer, A., Metzger, S., Stenchikov, G. L., and Lelieveld, J.: Aerosol optical depth trend over the Middle East, *Atmos. Chem. Phys.*, 16, 5063–5073, <https://doi.org/10.5194/acp-16-5063-2016>, 2016.
- Krom, M. D., Herut, B., and Mantoura, R. F. C.: Nutrient budget for the Eastern Mediterranean: Implications for phosphorus limitation, *Limnol. Oceanogr.*, 49, 1582–1592, <https://doi.org/10.4319/lo.2004.49.5.1582>, 2004.
- Krom, M. D., Emeis, K. C., and Van Cappellen, P.: Why is the Eastern Mediterranean phosphorus limited?, *Prog. Oceanogr.*, 85, 236–244, <https://doi.org/10.1016/j.pcean.2010.03.003>, 2010.
- Langlois, R. J., Hümmer, D., and LaRoche, J.: Abundances and Distributions of the Dominant nifH Phylotypes in the Northern Atlantic Ocean, *Appl. Environ. Microb.*, 74, 1922–1931, <https://doi.org/10.1128/AEM.01720-07>, 2008.
- Langlois, R. J., Mills, M. M., Ridame, C., Croot, P., and LaRoche, J.: Diazotrophic bacteria respond to Saharan dust additions, *Mar. Ecol. Prog. Ser.*, 470, 1–14, <https://doi.org/10.3354/meps10109>, 2012.
- Law, C. S., Breitbart, E., Hoffmann, L. J., McGraw, C. M., Langlois, R. J., LaRoche, J., Marriner, A., and Safi, K. A.: No stimulation of nitrogen fixation by non-filamentous diazotrophs under elevated CO<sub>2</sub> in the South Pacific, *Glob. Change Biol.*, 18, 3004–3014, <https://doi.org/10.1111/j.1365-2486.2012.02777.x>, 2012.
- Lazzari, P., Solidoro, C., Ibello, V., Salon, S., Teruzzi, A., Béranger, K., Colella, S., and Crise, A.: Seasonal and inter-annual variability of plankton chlorophyll and primary production in the Mediterranean Sea: a modelling approach, *Biogeosciences*, 9, 217–233, <https://doi.org/10.5194/bg-9-217-2012>, 2012.
- Le Moal, M., Collin, H., and Biegala, I. C.: Intriguing diversity among diazotrophic picoplankton along a Mediterranean transect: a dominance of rhizobia, *Biogeosciences*, 8, 827–840, <https://doi.org/10.5194/bg-8-827-2011>, 2011.
- Lekunberri, I., Lefort, T., Romero, E., Vázquez-Domínguez, E., Romera-Castillo, C., Marrasé, C., Peters, F., Weinbauer, M., and Gasol, J. M.: Effects of a dust deposition event on coastal marine microbial abundance and activity, bacterial community structure and ecosystem function, *J. Plankton Res.*, 32, 381–396, <https://doi.org/10.1093/plankt/fbp137>, 2010.
- Louis, J., Bressac, M., Pedrotti, M. L., and Guieu, C.: Dissolved inorganic nitrogen and phosphorus dynamics in abiotic seawater following an artificial Saharan dust deposition, *Front. Mar. Sci.*, 2, 27, <https://doi.org/10.3389/fmars.2015.00027>, 2015.
- Manca, B., Burca, M., Giorgetti, A., Coatanoan, C., Garcia, M.-J., and Iona, A.: Physical and biochemical averaged vertical profiles in the Mediterranean regions: An important tool to trace the climatology of water masses and to validate incoming data from operational oceanography, *J. Marine Syst.*, 48, 83–116, <https://doi.org/10.1016/j.jmarsys.2003.11.025>, 2004.
- Man-Aharonovich, D., Kress, N., Bar Zeev, E., Berman-Frank, I., and Beja, O.: Molecular ecology of nifH genes and transcripts in the Eastern Mediterranean Sea, *Environ. Microbiol.*, 9, 2354–2363, <https://doi.org/10.1111/j.1462-2920.2007.01353.x>, 2007.
- Marañón, E., Van Wambeke, F., Uitz, J., Boss, E. S., Dimier, C., Dinasquet, J., Engel, A., Haëntjens, N., Pérez-Lorenzo, M., Taillandier, V., and Zäncker, B.: Deep maxima of phytoplankton biomass, primary production and bacterial production in the Mediterranean Sea, *Biogeosciences*, 18, 1749–1767, <https://doi.org/10.5194/bg-18-1749-2021>, 2021.
- Martinez-Perez, C., Mohr, W., Loscher, C. R., Dekaezemacker, J., Littmann, S., Yilmaz, P., Lehnen, N., Fuchs, B. M., Lavik, G., Schmitz, R. A., LaRoche, J., and Kuypers, M. M.: The small unicellular diazotrophic symbiont, UCYN-A, is a key player in the marine nitrogen cycle, *Nat. Microbiol.*, 1, 16163, <https://doi.org/10.1038/nmicrobiol.2016.163>, 2016.
- Mas, J. L., Martin, J., Pham, M. K., Chamizo, E., Miquel, J.-C., Osvath, I., Povinec, P. P., Eriksson, M., and Villa-Alfageme, M.: Analysis of a major Aeolian dust input event and its impact on element fluxes and inventories at the DYFAMED

- site (Northwestern Mediterranean), *Mar. Chem.*, 223, 103792, <https://doi.org/10.1016/j.marchem.2020.103792>, 2020.
- Mermex Group, De Madron, X. D., Guieu, C., Sempere, R., Conan, P., Cossa, D., D'Ortenzio, F., Estournel, C., Gazeau, F., Rabouille, C., Stemmann, L., Bonnet, S., Diaz, F., Koubbi, P., Radakovitch, O., Babin, M., Baklouti, M., Bancon-Montigny, C., Belviso, S., Bensoussan, N., Bonsang, B., Bouloubassi, I., Brunet, C., Cadiou, J. F., Carlotti, F., Chami, M., Charmasson, S., Charriere, B., Dachs, J., Doxaran, D., Dutay, J. C., Elbaz-Poulichet, F., Eleaume, M., Eyrolles, F., Fernandez, C., Fowler, S., Francour, P., Gaertner, J. C., Galzin, R., Gasparini, S., Ghiglione, J. F., Gonzalez, J. L., Goyet, C., Guidi, L., Guizien, K., Heimbürger, L. E., Jacquet, S. H. M., Jeffrey, W. H., Joux, F., Le Hir, P., Leblanc, K., Lefevre, D., Lejeune, C., Leme, R., Loye-Pilot, M. D., Mallet, M., Mejanelle, L., Melin, F., Mellon, C., Merigot, B., Merle, P. L., Migon, C., Miller, W. L., Mortier, L., Mostajir, B., Mousseau, L., Moutin, T., Para, J., Perez, T., Petrenko, A., Poggiale, J. C., Prieur, L., Pujopay, M., Pulido, V., Raimbault, P., Rees, A. P., Ridame, C., Rontani, J. F., Pino, D. R., Sicre, M. A., Taillandier, V., Tamburini, C., Tanaka, T., Taupier-Letage, I., Tedetti, M., Testor, P., Thebault, H., Thouvenin, B., Touratier, F., Tronczynski, J., Ulses, C., Van Wambeke, F., Vantrepotte, V., Vaz, S., and Verney, R.: Marine ecosystems' responses to climatic and anthropogenic forcings in the Mediterranean, *Prog. Oceanogr.*, 91, 97–166, <https://doi.org/10.1016/j.pocean.2011.02.003>, 2011.
- Messer, L. F., Doubell, M., Jeffries, T. C., Brown, M. V., and Seymour, J. R.: Prokaryotic and diazotrophic population dynamics within a large oligotrophic inverse estuary, *Aquat. Microb. Ecol.*, 74, 1–15, <https://doi.org/10.3354/ame01726>, 2015.
- Mills, M. M., Turk-Kubo, K. A., van Dijken, G. L., Henke, B. A., Harding, K., Wilson, S. T., Arrigo, K. R., and Zehr, J. P.: Unusual marine cyanobacteria/haptophyte symbiosis relies on N<sub>2</sub> fixation even in N-rich environments, *ISME J.*, 14, 2395–2406, <https://doi.org/10.1038/s41396-020-0691-6>, 2020.
- Mohr, W., Grosskopf, T., Wallace, D. R. W., and LaRoche, J.: Methodological underestimation of oceanic nitrogen fixation rates, *PLoS One*, 5, 1–7, <https://doi.org/10.1371/journal.pone.0012583>, 2010.
- Moisander, P. H., Beinart, R. A., Hewson, I., White, A. E., Johnson, K. S., Carlson, C. A., Montoya, J. P., and Zehr, J. P.: Unicellular cyanobacterial distributions broaden the oceanic N<sub>2</sub> fixation domain, *Science*, 327, 5972, 1512–1514, <https://doi.org/10.1126/science.1185468>, 2010.
- Moisander, P. H., Serros, T., Paerl, R. W., Beinart, R. A., Zehr, J. P.: Gammaproteobacterial diazotrophs and nifH gene expression in surface waters of the South Pacific Ocean, *ISME J.*, 8, 1962–1973, <https://doi.org/10.1038/ismej.2014.49>, 2014.
- Montoya, J. P., Voss, M., Kahler, P., and Capone, D. G.: A simple, high-precision, high-sensitivity tracer assay for N<sub>2</sub> fixation, *Appl. Environ. Microb.*, 62, 986–993, <https://doi.org/10.1128/AEM.62.3.986-993.1996>.
- Moreira-Coello, V., Mouriño-Carballido, B., Marañón, E., Fernández-Carrera, A., Bode, A., and Varela, M. M.: Biological N<sub>2</sub> Fixation in the Upwelling Region off NW Iberia: Magnitude, Relevance, and Players, *Front. Mar. Sci.*, 4, 303, <https://doi.org/10.3389/fmars.2017.00303>, 2017.
- Moreira-Coello, V., Mouriño-Carballido, B., Marañón, E., Fernández-Carrera, A., Bode, A., Sintés, E., Zehr, J. P., Turk-Kubo, K., and Varela, M. M.: Temporal variability of diazotroph community composition in the upwelling region off NW Iberia, *Sci. Rep.-UK*, 9, 3737, <https://doi.org/10.1038/s41598-019-39586-4>, 2019.
- Moulin, C. and Chiapello, I.: Impact of human-induced desertification on the intensification of Sahel dust emission and export over the last decades, *Geophys. Res. Lett.*, 33, L18808, <https://doi.org/10.1029/2006GL025923>, 2006.
- Moynihan, M. A.: nifHdata2 GitHub repository, Zenodo, <https://doi.org/10.5281/zenodo.3958370>, 2020.
- Paerl, R. W., Hansen, T. N. G., Henriksen, N. S. E., Olesen, A. K., and Riemann, L.: N-fixation and related O<sub>2</sub> constraints on model marine diazotroph *Pseudomonas stutzeri* BAL361, *Aquat. Microb. Ecol.*, 81, 125–136, <https://doi.org/10.3354/ame01867>, 2018.
- Pierella Karlusich, J. J., Pelletier, E., Lombard, F., Carsique, M., Dvorak, E., Colin, S., Picheral, M., Cornejo-Castillo, F. M., Acinas, S. G., Pepperkok, R., Karsenti, E., de Vargas, C., Wincker, P., Bowler, C., and Foster, R. A.: Global distribution patterns of marine nitrogen-fixers by imaging and molecular methods, *Nat. Commun.*, 12, 4160, <https://doi.org/10.1038/s41467-021-24299-y>, 2021.
- Pulido-Villena, E., Wagener, T., and Guieu, C.: Bacterial response to dust pulses in the western Mediterranean: Implications for carbon cycling in the oligotrophic ocean, *Global Biogeochem. Cy.*, 22, GB1020, <https://doi.org/10.1029/2007GB003091>, 2008.
- Pulido-Villena, E., Rérolle, V., and Guieu, C.: Transient fertilizing effect of dust in P-deficient LNLC surface ocean, *Geophys. Res. Lett.*, 37, L01603, <https://doi.org/10.1029/2009GL041415>, 2010.
- Pulido-Villena, E., Baudoux, A.-C., Obernosterer, I., Landa, M., Caparros, J., Catala, P., Georges, C., Harmand, J., and Guieu, C.: Microbial food web dynamics in response to a Saharan dust event: results from a mesocosm study in the oligotrophic Mediterranean Sea, *Biogeosciences*, 11, 5607–5619, <https://doi.org/10.5194/bg-11-5607-2014>, 2014.
- Pulido-Villena, E., Desboeufs, K., Djaoudi, K., Van Wambeke, F., Barrillon, S., Doglioli, A., Petrenko, A., Taillandier, V., Fu, F., Gaillard, T., Guasco, S., Nunige, S., Triquet, S., and Guieu, C.: Phosphorus cycling in the upper waters of the Mediterranean Sea (PEACETIME cruise): relative contribution of external and internal sources, *Biogeosciences*, 18, 5871–5889, <https://doi.org/10.5194/bg-18-5871-2021>, 2021.
- Rahav, E., Herut, B., Levi, A., Mulholland, M. R., and Berman-Frank, I.: Springtime contribution of dinitrogen fixation to primary production across the Mediterranean Sea, *Ocean Sci.*, 9, 489–498, <https://doi.org/10.5194/os-9-489-2013>, 2013.
- Rahav, E., Shun-Yan, C., Cui, G., Liu, H., Tsagaraki, T. M., Giannakourou, A., Tsiola, A., Psarra, S., Lagaria, A., Mulholland, M. R., Stathopoulou, E., Paraskevi, P., Herut, B., and Berman-Frank, I.: Evaluating the impact of atmospheric depositions on springtime dinitrogen fixation in the Cretan Sea (eastern Mediterranean)—A mesocosm approach, *Front. Mar. Sci.*, 3, 180, <https://doi.org/10.3389/fmars.2016.00180>, 2016a.
- Rahav, E., Giannetto, J. M., and Bar-Zeev, E.: Contribution of mono and polysaccharides to heterotrophic N<sub>2</sub> fixation at the eastern Mediterranean coastline, *Sci. Rep.-UK*, 6, 27858, <https://doi.org/10.1038/srep27858>, 2016b.
- Rees, A. P., Law, C. S., and Woodward, E. M. S.: High rates of nitrogen fixation during an in-situ phosphate release experiment in

- the Eastern Mediterranean Sea, *Geophys. Res. Lett.*, 33, L10607, <https://doi.org/10.1029/2006GL025791>, 2006.
- Rees, A. P., Turk-Kubo, K. A., Al-Moosawi, L., Alliouane, S., Gazeau, F., Hogan, M. E. and Zehr, J. P.: Ocean acidification impacts on nitrogen fixation in the coastal western Mediterranean Sea, *Estuar. Coast. Shelf S.*, 186, 45–57, <https://doi.org/10.1016/j.ecss.2016.01.020>, 2017.
- Ridame, C., Le Moal, M., Guieu, C., Ternon, E., Biegala, I. C., L'Helguen, S., and Pujo-Pay, M.: Nutrient control of N<sub>2</sub> fixation in the oligotrophic Mediterranean Sea and the impact of Saharan dust events, *Biogeosciences*, 8, 2773–2783, <https://doi.org/10.5194/bg-8-2773-2011>, 2011.
- Ridame, C., Guieu, C., and L'Helguen, S.: Strong stimulation of N<sub>2</sub> fixation in oligotrophic Mediterranean Sea: results from dust addition in large in situ mesocosms, *Biogeosciences*, 10, 7333–7346, <https://doi.org/10.5194/bg-10-7333-2013>, 2013.
- Ridame, C., Dekaezemacker, J., Guieu, C., Bonnet, S., L'Helguen, S., and Malien, F.: Contrasted Saharan dust events in LNLC environments: impact on nutrient dynamics and primary production, *Biogeosciences*, 11, 4783–4800, <https://doi.org/10.5194/bg-11-4783-2014>, 2014.
- Robidart, J., Church, M., Ryan, J., Ascani, F., Wilson, S. T., Bombar, D., Marin III, R., Richards, K. J., Karl, D. M., Scholin, C. A., and Zehr, J. P.: Ecogenomic sensor reveals controls on N<sub>2</sub>-fixing microorganisms in the North Pacific Ocean, *ISME J.*, 8, 1175–1185, <https://doi.org/10.1038/ismej.2013.244>, 2014.
- Roy-Barman, M., Foliot, L., Douville, E., Leblond, N., Gazeau, F., Bressac, M., Wagener, T., Ridame, C., Desboeufs, K., and Guieu, C.: Contrasted release of insoluble elements (Fe, Al, rare earth elements, Th, Pa) after dust deposition in seawater: a tank experiment approach, *Biogeosciences*, 18, 2663–2678, <https://doi.org/10.5194/bg-18-2663-2021>, 2021.
- Sherr, E. B., Sherr, B. F., and Sigmon, C. T.: Activity of marine bacteria under incubated and in situ conditions, *Aquat. Microb. Ecol.*, 20, 213–223, 1999.
- Siokou-Frangou, I., Christaki, U., Mazzocchi, M. G., Montresor, M., Ribera d'Alcalá, M., Vaqué, D., and Zingone, A.: Plankton in the open Mediterranean Sea: a review, *Biogeosciences*, 7, 1543–1586, <https://doi.org/10.5194/bg-7-1543-2010>, 2010.
- Smith, D. C. and Azam, F.: A simple, economical method for measuring bacterial protein synthesis rates in sea water using 3H-Leucine, *Mar. Microb. Food Webs*, 6, 107–114, 1992.
- Somot, S., Sevault, F., Deque, M., and Crepon, M.: 21st century climate change scenario for the Mediterranean using a coupled atmosphere – ocean regional climate model, *Global Planet. Change*, 63, 112–126, <https://doi.org/10.1016/j.gloplacha.2007.10.003>, 2008.
- Tang, W., Wang, S., Fonseca-Batista, D., Dehairs, F., Gifford, S., Gonzalez, A. G., Gallinari, M., Planquette, H., Sarthou, G., and Cassar, N.: Revisiting the distribution of oceanic N<sub>2</sub> fixation and estimating diazotrophic contribution to marine production, *Nat. Commun.*, 10, 831, <https://doi.org/10.1038/s41467-019-08640-0>, 2019.
- Tegen, I., Werner, M., Harrison, S. P., and Kohfeld, K. E.: Relative importance of climate and land use in determining present and future global soil dust emissions, *Geophys. Res. Lett.*, 31, L05105, <https://doi.org/10.1029/2003GL019216>, 2004.
- Ternon, E., Guieu, C., Ridame, C., L'Helguen, S., and Catala, P.: Longitudinal variability of the biogeochemical role of Mediterranean aerosols in the Mediterranean Sea, *Biogeosciences*, 8, 1067–1080, <https://doi.org/10.5194/bg-8-1067-2011>, 2011.
- Thompson, A., Carter, B. J., Turk-Kubo, K., Malfatti, F., Azam, F., and Zehr, J. P.: Genetic diversity of the unicellular nitrogen-fixing cyanobacteria UCYN-A and its prymnesiophyte host, *Environ. Microbiol.*, 16, 3238–3249, <https://doi.org/10.1111/1462-2920.12490>, 2014.
- Thompson, A. W., Foster, R. A., Krupke, A., Carter, B. J., Musat, N., Vaultot, D., Kuypers, M. M. M., and Zehr, J. P.: Unicellular cyanobacterium symbiotic with a single-celled eukaryotic alga, *Science*, 337, 1546–1550, <https://doi.org/10.1126/science.1222700>, 2012.
- Tovar-Sánchez, A., Rodríguez-Romero, A., Engel, A., Zäncker, B., Fu, F., Marañón, E., Pérez-Lorenzo, M., Bressac, M., Wagener, T., Triquet, S., Siour, G., Desboeufs, K., and Guieu, C.: Characterizing the surface microlayer in the Mediterranean Sea: trace metal concentrations and microbial plankton abundance, *Biogeosciences*, 17, 2349–2364, <https://doi.org/10.5194/bg-17-2349-2020>, 2020.
- Tripp, H. J., Bench, S. R., Turk, K. A., Foster, R. A., Desany, B. A., Niazi, F., Affourtit, J. P., and Zehr, J. P.: Metabolic streamlining in an open-ocean nitrogen-fixing cyanobacterium, *Nature*, 464, 90–94, <https://doi.org/10.1038/nature08786>, 2010.
- Tuit, C., Waterbury, J., and Ravizza, G.: Diel variation of molybdenum and iron in marine diazotrophic cyanobacteria, *Limnol. Oceanogr.*, 49, 978–990, <https://doi.org/10.4319/lo.2004.49.4.0978>, 2004.
- Turk-Kubo, K. A., Karamchandani, M., Capone, D. G., and Zehr, J. P.: The paradox of marine heterotrophic nitrogen fixation: abundances of heterotrophic diazotrophs do not account for nitrogen fixation rates in the Eastern Tropical South Pacific, *Environ. Microbiol.*, 16, 3095–3114, <https://doi.org/10.1111/1462-2920.12346>, 2014.
- Turk-Kubo, K. A., Farnelid, H. M., Shilova, I. N., Henke, B., and Zehr, J. P.: Distinct ecological niches of marine symbiotic N<sub>2</sub>-fixing cyanobacterium *Candidatus Atelocyanobacterium thalassa* sublineages, *J. Phycol.*, 53, 2, 451–461, <https://doi.org/10.1111/jpy.12505>, 2017.
- Van Wambeke, F., Taillandier, V., Desboeufs, K., Pulido-Villena, E., Dinasquet, J., Engel, A., Marañón, E., Ridame, C., and Guieu, C.: Influence of atmospheric deposition on biogeochemical cycles in an oligotrophic ocean system, *Biogeosciences*, 18, 5699–5717, <https://doi.org/10.5194/bg-18-5699-2021>, 2021.
- Wang, Q., Quensen, J. F., Fish, J. A., Lee, T. K., Sun, Y., Tiedje, J. M., and Cole, J. R.: Ecological patterns of nifH genes in four terrestrial climatic zones explored with targeted metagenomics using FrameBot, a new informatics tool, *MBio*, 4, e00592-13, <https://doi.org/10.1128/mBio.00592-13>, 2013.
- Webb, E. A., Ehrenreich, I. A., Brown, S. L., Valois, F. W., and Waterbury, J. B.: Phenotypic and genotypic characterization of multiple strains of the diazotrophic cyanobacterium, *Crocospaera watsonii*, isolated from the open ocean, *Environ. Microbiol.*, 11, 2, 338–348, <https://doi.org/10.1111/j.1462-2920.2008.01771.x>, 2008.
- Yogev, T., Rahav, E., Bar-Zeev, E., Man-Aharonovich, D., Stambler, N., Kress, N., Béjà, O., Mulholland, M. R., Herut, B., and Berman-Frank, I.: Is dinitrogen fixation significant in the Levantine Basin, East Mediterranean Sea?, *Environ. Microbiol.*, 13,

- 4, 854–871, <https://doi.org/10.1111/j.1462-2920.2010.02402.x>, 2011.
- Zehr, J. P., Mellon, M. T., and Zani, S.: New nitrogen fixing microorganisms detected in oligotrophic oceans by the amplification of nitrogenase (*nifH*) genes, *Appl. Environ. Microb.*, 64, 3444–3450, <https://doi.org/10.1128/AEM.64.9.3444-3450.1998>, 1998.
- Zehr, J. P., Bench, S. R., Carter, B. J., Hewson, I. and Nizazi, F.: Globally Distributed Uncultivated Oceanic N<sub>2</sub>-Fixing Cyanobacteria Lack Oxygenic Photosystem II, *Science*, 322, 1110, <https://doi.org/10.1126/science.1165340>, 2008.